FOSR FINAL SCIENTIFIC REPORT
FOSR 70-1873TR

DS TR-A-70-103

# COMBUSTION CHEMISTRY AND MIXING IN SUPERSONIC FLOW



STUART HERSH
MELVIN GERSTEIN

SEPTEMBER 1970

PREPARED FOR: HEADQUARTERS
AIR FORCE OFFICE OF SCIENTIFIC RESEARCH
OFFICE OF AEROSPACE RESEARCH
UNITED STATES AIR FORCE
WASHINGTON 25, D. C.

**DYNAMIC SCIENCE**
A Division of Marshall Industries
2400 Michelson Drive, Irvine, California 92664 (714) 833-2670



"1. This document has been approved for public release and sale; its distribution is unlimited."

# COMBUSTION CHEMISTRY AND MIXING IN SUPERSONIC FLOW

Final Report Number DS TR-A-70-103

Prepared for: Headquarters
Air Force Office of Scientific Research
Office of Aerospace Research
United States Air Force
Washington 25, D. C.

Prepared by: Stuart Hersh
Melvin Gerstein

16 September 1970

DYNAMIC SCIENCE
2400 Michelson Drive
Irvine, California

## ABSTRACT

Analytical and experimental investigations of the ignition and combustion of hydrogen-oxygen-argon mixtures are presented. A one-dimensional kinetics program with generalized chemistry and provisions for mass addition, momentum addition, heat loss, mixing, shock waves, and a rate screening option has been developed and used to analyze the effect of free radical additives on the ignition delay time in hydrogen-oxygen mixtures. This computer program has also been used to reduce shock tube measurements of hydrogen-oxygen ignition delay and $OH\ ^2\Sigma - {}^2\Pi$ emission. The experimental results indicate that the reaction O + H (+ M) → OH* (+ M) is responsible for producing OH ($^2\Sigma$) during the induction period; however, this mechanism, when input into the computer program, was not sufficient to qualitatively reproduce OH emission intensity profiles obtained experimentally. Work aimed at determining the mechanism for OH emission throughout the reaction zone is continuing.

TABLE OF CONTENTS

# I. INTRODUCTION

Combustion in a supersonic stream has become one of the most important new approaches to achieving hypersonic flight with air breathing engine systems. In the past few years, a considerable amount of effort has been expended in theoretical analysis of the combustion process and in the design of hardware. A number of fundamental questions still remain unresolved, however. These questions, pertaining to the mechanism of ignition and reaction in a rapidly mixing fuel-air system, the establishment of suitable reaction rate expressions under conditions where reaction and mixing occur at competitive rates, and the effect of additives on the chemically reacting system, are still essential and yet unresolved problems.

This report describes the work conducted under AFOSR Contract No. F44620-68-C-0069 to gain insight into these fundamental processes. This work is being continued under AFOSR Contract No. F44620-70-C-0061.

Analytical investigations of ignition and combustion and the effect of additives on ignition delay were carried out for the hydrogen-oxygen system using an existing one-dimensional chemical kinetics computer program significantly modified to include generalized chemistry, mass addition, momentum addition, heat loss, mixing, shock waves, and the capability of conducting a chemical rate screening analysis.

An experimental program was conducted in order to better understand the details of the complex chemical processes occurring during ignition and combustion. The portion of the experimental program completed to date consists of measurement of $OH\ ^2\Sigma - {}^2\Pi$ emission for both the ignition zone and the entire combustion zone. These measurements were used to determine the ignition delay times and are currently being examined in conjunction with the computer program to deduce the mechanism that produces excited OH.

## II. TECHNICAL DISCUSSION

### COMPUTER PROGRAM DEVELOPMENT

At the outset of this program, it was decided that the development of a complex computer program which treated the fluid mechanical details of turbulent mixing and diffusion in as exact a manner as is possible by the current state-of-the-art would be both duplicative (several programs of this type are currently in existence, for example, Reference 1), and beyond the scope of our particular line of investigation; therefore, it was decided to develop an analysis which treated the chemical kinetics exactly and had provisions for mass transfer, heat tranfer and momentum addition in a simplified manner. Above all, this program would be simple to use, require a minimum of computer time, and be easily adaptable to handle diverse problems. It was envisioned that this tool would find its maximum usefulness during the development and testing stage of actual scramjet hardware. These objectives have been achieved.

The computer program utilizes the JANNAF (ICRPG) One-Dimensional Kinetics Program as a framework to which significant modifications were added, greatly enhancing its capabilities as a diagnostic tool. The major features of the program, as it presently exists, are briefly enumerated below, and a detailed description of the program mechanics can be found in Appendix A.

1. The method of solution has been modified to allow the integration of the conservation equations for the chemical system in a form such that the chemistry is generalized. This generalized chemistry feature allows the user to easily input up to 40 species and 158 reactions in symbolic form, including specified third body efficiencies for each reaction, if necessary. The JANNAF thermochemical data is available as part of the program in a form which allows for future expansion directly from the JANNAF format.

2. The fully implicit numerical integration method used in the program makes it the most efficient program of its type, particularly when handling chemical systems near equilibrium or in an ignition region. It has been shown that explicit methods of numerical integration are unstable when applied to relaxation equations unless the integration step size is of the order of the characteristic relaxation distance. Since in the near equilibrium flow regime the characteristic relaxation distance is typically many orders of magnitude smaller than characteristic physical dimensions of the system of interest, the use of explicit methods to integrate relaxation equations often results in excessively long computation times. An implicit integration method which is inherently stable in all flow situations (whether near equilibrium or frozen) is therefore used by the computer program. With this method, step sizes which are of the order of the physical dimensions of the system of interest can be used, reducing the computation time and cost per case several orders of magnitude when compared with conventional explicit integration methods.

3. Mass, momentum, and energy addition rates can be specified as part of the initial input conditions.

4. Finite mixing times are accounted for by holding back a portion of the initial fuel from reaction, until after a finite "mixing time" or, when a specified axial position is reached.

5. If shock waves exist at known locations in the flow, the program will consider them exactly if the program input contains either the downstream pressure, velocity or the shock angle.

6. The program has also been modified so as to make available a unique analysis capability for complex reacting systems. At the desire of the user the program will print out, in increasing

order, the quantitative contribution of each reaction to the production of any of the species taking part in the reacting system. The program will then eliminate from the reaction set those reactions whose relative contribution to the production of any specie falls below a preset level. The integration step is then recomputed with the reduced reaction set and all parameters printed out along with the original computation for comparison.

It should be emphasized that one of the most significant features of this program is its operating efficiency. While a number of options are available which makes the program an extremely flexible tool, the required information needed to automate any particular option is straightforward and can be input easily. In addition, the program's very low operating costs per computer run make it ideal for use when a large number of cases must be run, for example, during the development and testing stage of actual hardware.

## ADDITIVE EFFECTIVENESS STUDIES

A theoretical study of the effect of additives on the ignition delay of the hydrogen-oxygen reaction has been presented in Reference 2. Since that work was presented, the program was further modified by the addition of a reaction screening option which allowed an even more detailed investigation of the entire reaction process. Using this option, it is possible to print out the specific contribution of each reaction in the chemical system toward the production of each of the species that exist in the system. This data immediately pinpoints the dominant reaction or reactions at any time during the chemical process. This information must be available if reaction rate constants, or reaction mechanisms are to be obtained from experimental measurements made during a chemical process involving a multitude of individual reactions.

Figure 1 which plots the rate of production or destruction of hydrogen atoms for each reaction versus time for given initial conditions, illustrates the ease with which the details of the chemical process can be seen by this type of presentation. From this figure it can be seen that the production of the dominant chain carrier (H atoms) during the induction period of the hydrogen-oxygen reaction, is controlled by the three reactions

$$H_2 + OH = H_2O + H$$

$$H_2 + O = OH + H$$

$$O_2 + H = OH + O$$

In addition, the transition of the hydrogen dissociation reaction $H_2 \rightarrow 2H$, to a recombination reaction $H + H \rightarrow H_2$, can be seen to occur at approximately 65 microseconds with a similar reversal occurring for the reaction $O_2 + H \rightarrow HO_2$ at 125 microseconds. The chemical mechanism which was used for this calculation is given in Table 1.

It is in the region past "ignition" when the contribution of several reactions to the production of H atoms are the same order of magnitude, that the screening option of the program is particularly useful. If another run is made with the same initial conditions but with a modified reaction rate parameter for a particular reaction, the effect of this perturbed rate on the total reaction picture will become readily apparent. This option, therefore, can be used to set limits within which rate parameters must be known in order to have a particular degree of confidence in the computed results. The program can also be used to establish physical conditions for which reactions whose rate parameters are poorly known and possibly difficult or impossible to measure in an isolated system, are dominant and control the variation of a readily measured physical property of the complex system, e.g., another specie concentration, T, $\rho$, etc. Experiments can then be conducted at these conditions to yield data which can be directly and quantitatively linked to the unknown reaction rate.

The screening option was used to investigate the details underlying the effectiveness of free radical producing additives in reducing ignition delay. Figure 2 shows the results of 2 calculations for identical initial conditions except for $6 \times 10^{-8}$ mole fraction of H atoms added for the second calculation. As can be seen, the effect of this "additive" on the ignition and combustion process is to shift the production curve toward earlier times. In fact, the magnitude of this time shift is just the time that it takes the reactions alone to produce a $6 \times 10^{-8}$ mole fraction of H atoms. While this result may appear to be obvious, it is significant to observe that no shifts in reaction mechanism, or in the dominance of any particular reaction, have been effected by the inclusion of the additive. Therefore, by making one analytical calculation, it is possible to know exactly what concentration of additive must be added initially in order to achieve a particular reduction in ignition delay time.

The above conclusion will not, of course, be valid for very large additive concentrations, and the limiting concentration below which these results are applicable is currently being determined.

Experimental verification of this phenomena is planned for future investigation.

## EXPERIMENTAL STUDIES

The experimental portion of this program was undertaken to provide data to verify the predictions of the analytical model, and to develop empirical relations which could be used to specify the mixing times or lengths required as input by the computer program. The original plan for this test program involved monitoring the concentrations of several chemical species during the ignition and combustion process. For ignition delay studies, a measurement of the concentration of OH would be sufficient to determine the characteristics of the combustion process for hydrogen-oxygen. However, for fuels other than hydrogen, and in particular, the planned mixing zone experiments, it was desirable to monitor simultaneously the concentration of two or more species. Spectroscopic absorption measurements have been widely

used to quantitatively measure species concentration in reacting gas mixtures. However, because of the difficulty involved in making simultaneous absorption measurements at different wave lengths, and because the experimental simplicity of emission measurements would enhance their use for examining a multitude of combustion processes, it was decided to use a measurement of the emitted band radiation as an indication of the progress of the chemical reactions.

A description of the shock tube facility in which the experiments were conducted is given in Reference 2 and is included in this report for completeness.

In operation, test samples are prepared manometrically and fed into the driven section of the tube through a port in the test section. During the check-out phase of the facility, it was found that the burst pressure of the shock tube diaphragm could be held to within 1% when a large number of diaphragms were identically scribed on a milling machine. Throughout the experimental study, the procedure adopted was to select a diaphragm material, thickness and scribe depth which would have optimum opening characteristics at a desired burst pressure. A range of shock speeds were then obtained by replacing a portion of the hydrogen driver gas with nitrogen. Varying the molecular weight of the driver gas in this manner, provided accurate control of the incidence shock velocity throughout a $1000^{\circ}K$ variation in temperature behind the shock wave.

The shock velocity was determined by displaying amplified outputs from platinum thin film gauges (located at intervals along the tube) on a rastered sweep displayed on a Tectronix type 556 oscilloscope. The raster was intensity modulated by a Tectronix type 184 time mark generator, giving shock wave transit times between gauges that were measurable to within one microsecond. After a preset delay time provided by the internal delay generator on the 556, a Tectronix type 533A oscilloscope was triggered which displayed the output of an EMI 9601B photomultiplier tube (S-11(C)) extended range photocathode which monitored the $^2\Sigma - {}^2\Pi$ band radiation from the OH molecule through a Hilger-Engis Model 600 monochrometer-spectrometer. Coincident with the triggering of the type 533A oscilloscope, a signal is imposed on the raster sweep thereby providing for timing correlation between the shock position and the ignition trace. Sample oscilloscope outputs are shown in Figures 3, 4.

The ignition delay is computed by measuring the time between the last heat tranfer signal and the initiation of the type 533A trace. To this time is added the time interval between the start of the type 533A trace and the first appearance of an emission signal, measured directly from the photomultiplier output trace. The time it takes the shock wave to travel from the last heat transfer gauge to the observation station is calculated from the measured shock wave velocity and then subtracted from the above sum. The ignition delay is then determined by multiplying this time by the shock wave density ratio to convert from laboratory time to particle time. The appearance of the timing marks simultaneously on both oscilloscopes helps to considerably reduce data reduction errors.

The use of emitted radiation as a characteristic of the initiation and progress of a chemically reacting system also presents several difficulties, particularly if one is interested in radiation from the OH molecule. At the temperatures of interest, almost all of the OH is in the electronic groundstate, and absorption measurements can be directly and quantitatively related to the concentration of OH. It has been amply demonstrated that below 2000°K the mechanism for emitted OH radiation is chemiluminescent in nature (Refs. 3, 4 ). Therefore, before it is possible to realte OH emission to a specific chemical composition, it is necessary to know the exact chemical mechanism by which electronically excited OH is produced.

The reactions which are sufficiently energetic to produce OH in the $^2\Sigma$ state are listed in Table 2. During the preignition phase of the hydrogen-oxygen reaction, the concentrations of the free radicals, O, OH, and H grow exponentially with the form

$$[O] = [O]_0 \, e^{\alpha t}$$

$$[H] = [H]_0 \, e^{\alpha t}$$

$$[OH] = [OH]_0 \, e^{\alpha t}$$

References 3,5 have shown that during this exponential growth period, the emission intensity from OH takes the form $I = I_0 e^{n\alpha t}$ where n is the number of free radicals taking part in the excitation reaction. Therefore, comparing values of the OH emission time constant with the time constant for the growth of any of the free radicals will determine n. The experimental results presented in Ref. 3, which compare the growth constant for OH emission with that of OH absorption, and Ref. 4, where the more sensitive end-on technique was used to compare the growth constant for OH emission with the growth constant of emission resulting from the O-CO reaction, indicate that the value for n is 2. Further, the most probable reaction which involves 2 free radicals and produces excited OH was concluded by both authors to be $O + H + (M) = OH^* + (M)$. Neither author was able to conclusively demonstrate whether this reaction required a third body or not.

The result of the more sensitive of our experiments are shown in Figure 5 which compares measured growth constants for OH emission with theoretical calculations of the free radical growth constant obtained using the reaction mechanism given in Table 1. The factor of 2 difference between our experimental and theoretical calculations tends to corroborate the 2 free radical reaction mechanisms proposed in References 3 and 4. However, using this mechanism we have been unable to analytically reproduce qualitative emission intensity profiles which agree with those obtained experimentally throughout the entire combustion region. This inability to analytically reproduce the experimental results cannot be explained by introducing a quenching mechanism and therefore indicate either a shifting chemical mechanism for producing excited OH once the ignition transients are passed or significant third body effects which come into play as the reaction proceeds.

All of the intensity profiles exhibited a sudden shift in emission growth rate at some time after ignition. This shift is barely perceptible at the high temperatures ($\sim 2000^\circ K$) and becomes quite pronounced as the temperature decreases. The appearance of this "shoulder" has been observed in OH emission profiles in high temperature methane-oxygen mixtures under similar test conditions, i.e., high argon dilution, $T < 2000^\circ K$, by Bowman and Seery (Ref. 7). They proposed that the chemiluminescent reaction producing excited OH during hydrocarbon oxidation is

$$CH(^2\Pi) + O_2(^3\Sigma_s) \rightarrow CO(^1\Sigma^+) + OH(^2\Sigma^+)$$

and the shoulder is caused by the competition for CH between this reaction and

$$C(^3P) + CH(^2\Pi) \rightarrow C_2(^3\Pi_g) + H(^2S)$$

This conclusion was supported by their experiments which showed a rapid increase in $C_2$ starting at the time the OH emission shoulder was reached.

A number of the tests in the present study were rerun with the hydrogen replaced by argon in an attempt to determine if some hydrocarbon contaminant was responsible for a portion of the measured OH emission profile, including the shoulder. No emission was measured in these tests.

In view of these results and those of References 3 and 4 in regard to the mechanism of OH chemiluminescence in $H_2$-$O_2$ systems, it appears that in the present case the "shoulder" is due either to a reaction involving O or H becoming prominent, or a complete change in the chemiluminescent reaction. These possibilities are currently being investigated.

The OH emission intensity profiles were also used to measure "ignition delay time" (defined as the first appearance of an emission signal) for the hydrogen-oxygen reaction as described above. This data was used to: compare results from our new facility with experimental results obtained by other investigators; to verify the ignition delay time predictions of the computer analysis with experimentally measured delay times; and to provide base runs for additive effectiveness experiments. Figure 7 compares experimentally measured ignition delay time for a $H_2/O_2 = 1$ mixture ratio with the analytically predicted ignition delay times determined by the computer program. The correlation used is that proposed in Ref. 6. As can be seen, the analytical predictions are in excellent agreement with the experimental measurements. Experiments are currently being planned to provide data on additive effectiveness for comparison with the analytically obtained effects of additive addition.

TABLE 1

CHEMICAL REACTIONS USED IN COMPUTATIONS
(REVERSE RATE PARAMETERS $k_{Rev} = AT^{-N} e^{-B/RT}$

```
H2       = H + H  ,    A=8.00E17,   N=1.0,    B=0.0,
O2       = O + O  ,    A=1.90E16,   N=0.5 ,   B=0.0   ,
H2O      = OH + H ,    A=1.17E17,   N=0.0,    B=0.0   ,   LEEDS 2 VQ
HO2      = O2 + H ,    A=1.59E15,   N=0.0 ,   B=-1.0  ,   LEEDS 3
OH       = O + H  ,    A=2.00E18,   N=1.0 ,   B=0.0   ,
OH + OH = H2O2    ,    A=1.17E17,   N=0.0 ,   B=+5.5  ,   LEEDS 3  Q
OHX + PHOTON = O+ H,   A=1.00E14,   N=0.0,    B=0.0   ,
END TBR REAX
H2O + H = H2 + OH ,    A=2.19E13,   N=0.0 ,   B=5.15  ,   LEEDS 2
OH + H  = H2 + O  ,    A=1.74E13,   N=0.0,    B=9.45,     LEEDS 2
OH + O  = O2 + H  ,    A=3.00E14,   N=0.0,    B=16.8,
OH + OH = H2O + O ,    A=5.75E13,   N=0.0 ,   B=18.0  ,   LEEDS 2 VQ
H2O + HO2 = H2O2 + OH, A=1.00E13,   N=0.0 ,   B=1.8   ,   LEEDS 3  R
 H2O2 + H = H2 + HO2,  A=9.60E12,   N=0.0 ,   B=24.0  ,   LEEDS 3R
OH + PHOTON = OHX ,    A=1.8E6,     N=0.0,     B=0.0,
```

TABLE 2

POSSIBLE OH ($^2\Sigma$) PRODUCTION REACTIONS ($\Delta E$ = 88 Kcal/mole)

$$H + H + OH \rightarrow OH^* + H_2$$

$$O + O + OH \rightarrow OH^* + O_2$$

$$H + OH + OH \rightarrow OH^* + H_2O$$

$$O + H_2 + OH \rightarrow OH^* + H_2O$$

$$H + O_2 + H_2 \rightarrow OH^* + H_2O$$

$$O + H\,(+M) \rightarrow OH^*\,(+M)$$

OH* DESTRUCTION REACTIONS

$$OH^* + M \rightarrow OH + M$$

$$OH^* \rightarrow OH + h\nu$$

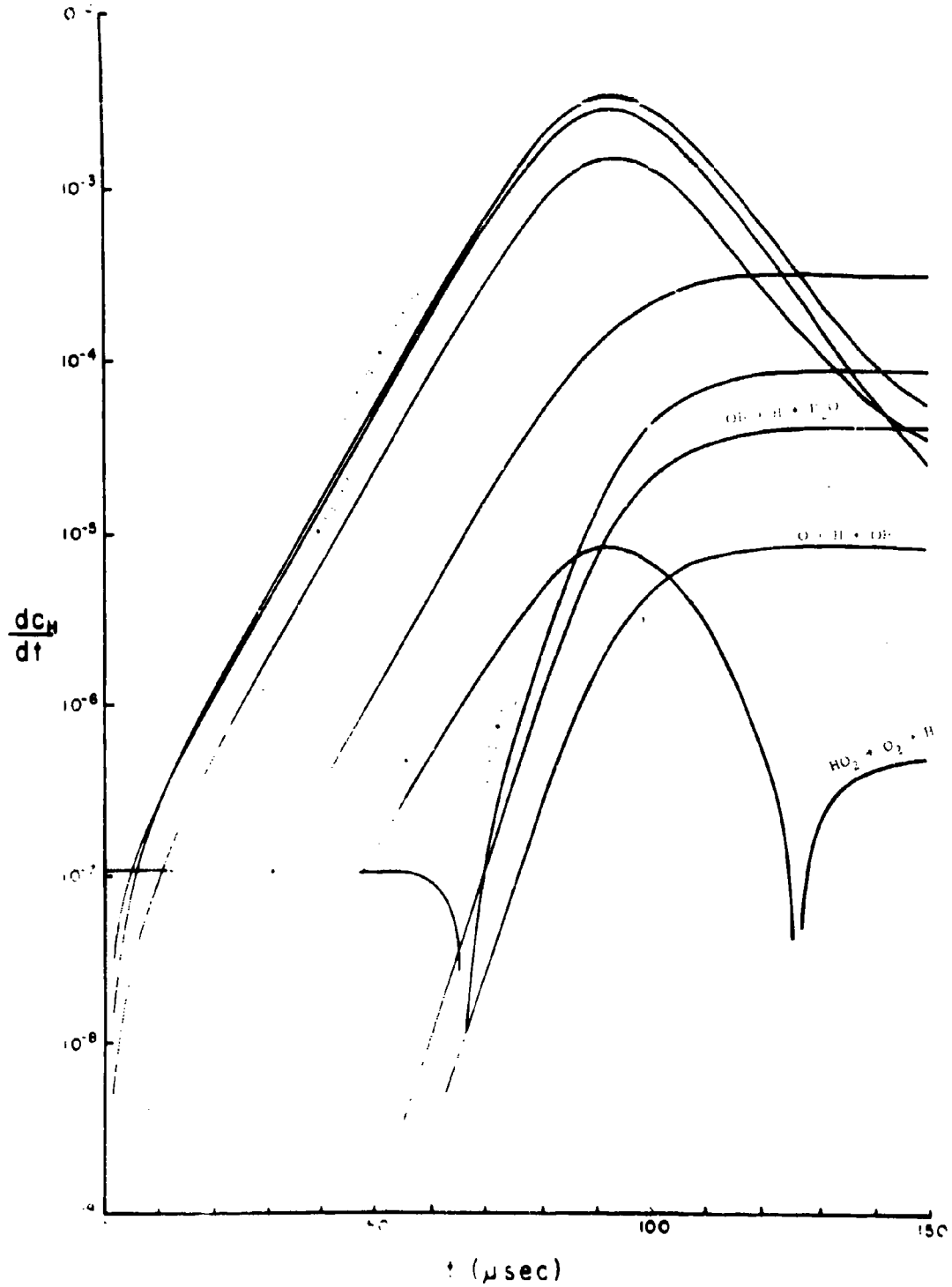


Figure 1. Individual Reaction H Atoms Production Rate
$H_2/O_2 = 1$

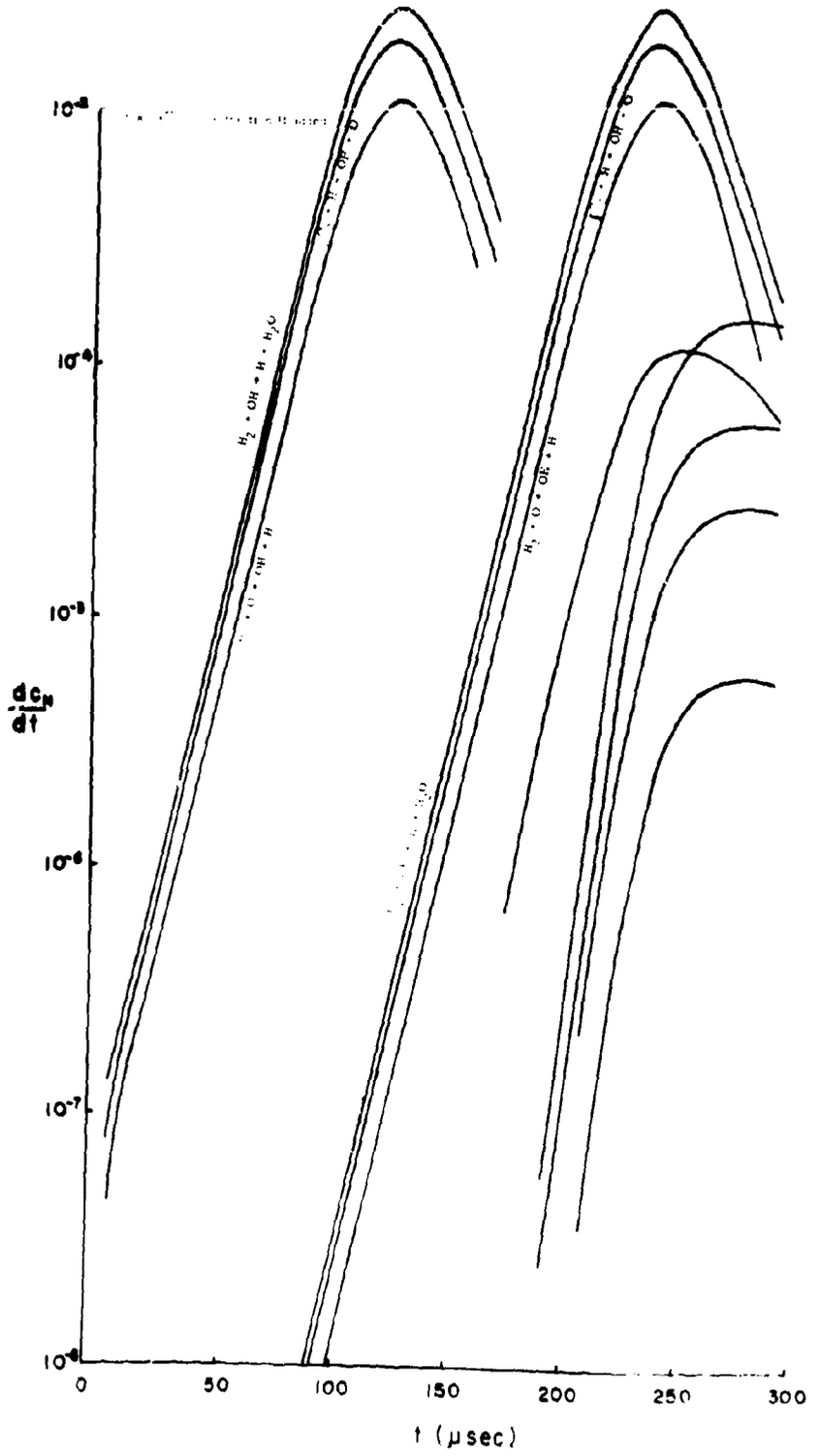


Figure 2. Effect of Adding H Atoms on Reaction Production Rates $H_2/O_2 = 1$

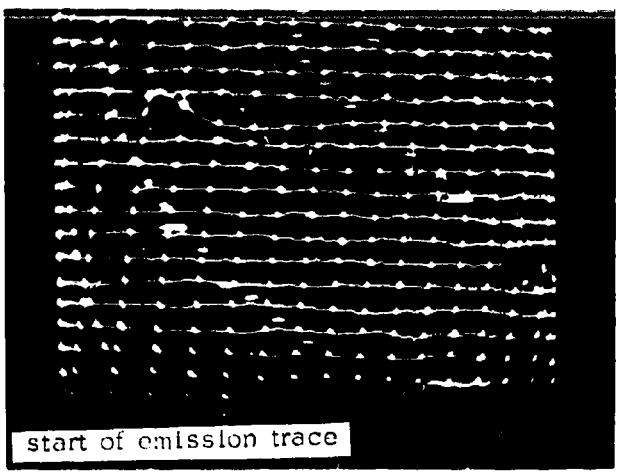


Figure 3. Shock Speed Trace

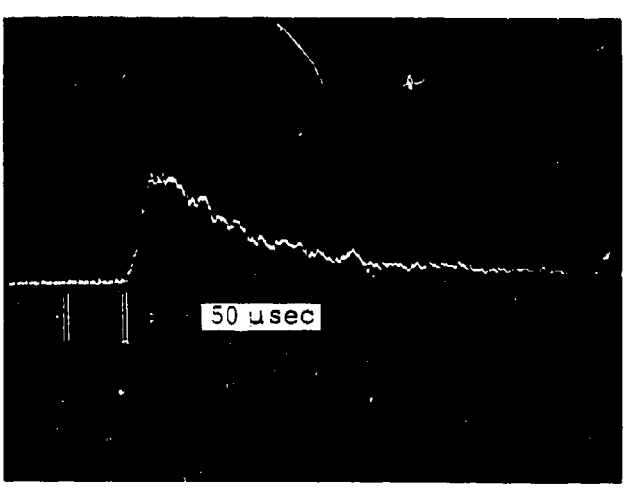


Figure 4. Emission Trace

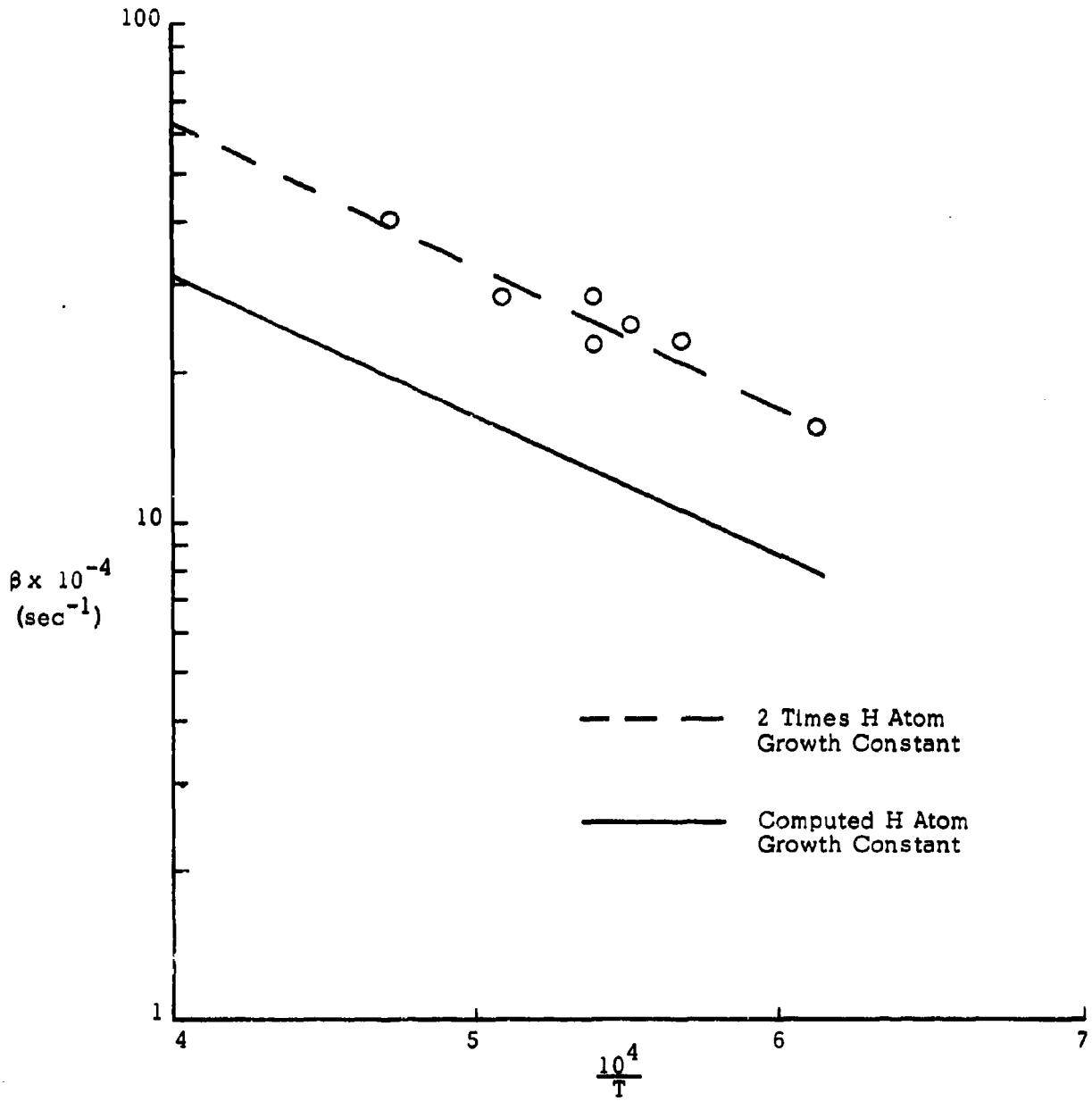


Figure 5. Emission Growth Constant

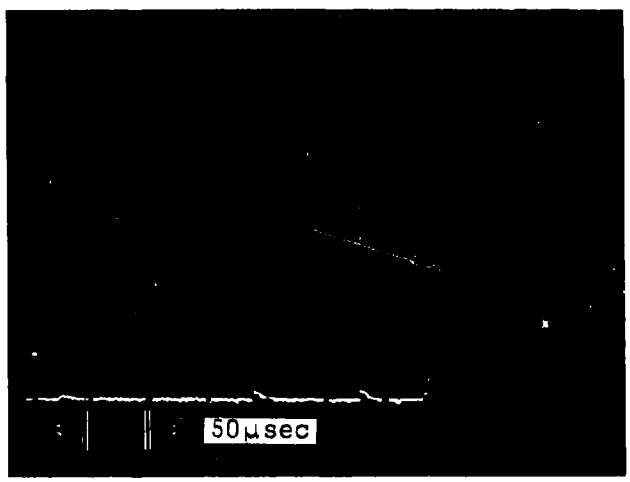


Figure 6. Emission Growth Rate Transition

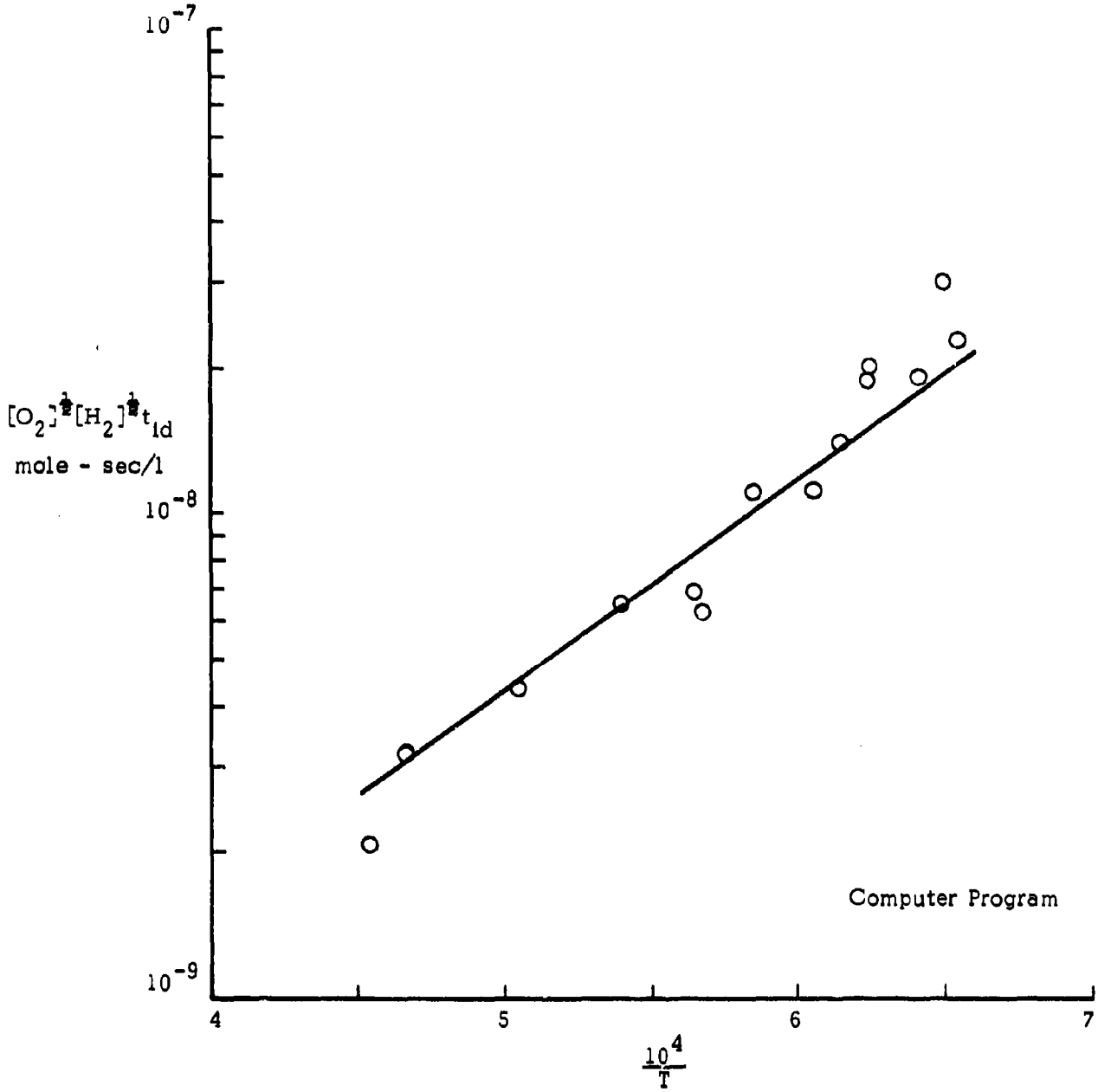


Figure 7. Ignition Delay Time
$H_2/O_2 = 1$

# APPENDIX A

# COMPUTER PROGRAM

## APPENDIX A

### 1. ANALYSIS

The computer program described in this report is based on analysis developed previously by the authors for the purpose of predicting delivered specific impulse, including the effect of kinetic losses, for liquid propellant rocket engines. Results of these earlier efforts are reported in references 1-3. This computer program has been written for the purpose of screening and analyzing generalized kinetic processes. The method of solution consists of integrating the conversation equations for the chemical system in a form such that the chemistry is generalized for binary exchange and dissociation-recombination reactions. Solid or liquid phase products are not considered.

#### Conservation Equations

The SCREEN computer program integrates a set of simultaneous differential equations along a pressure defined streamtube (i.e., P(x) and dP(x)/dx are known). These differential equations represent the conservation of species, mass, momentum, and energy for the system as expressed by equations (5), (6), (7), and (8) below.

The conservation equations governing the inviscid flow of reacting gas mixtures have been given by Hirschfelder, Curtiss, and Bird[4], Penner[5] and others. The following basic assumptions are made in the derivation of these equations.

- Mass ($\dot{m}$, $\dot{s}_i$), momentum ($\dot{M}$), and energy ($\dot{H}$) addition rates are defined for the system.
- The gas is inviscid.
- Each component of the gas is a perfect gas.
- The internal degrees of freedom of each component of the gas are in equilibrium.

In one-dimensional flow, the conservation equations have the form*

species $$\frac{d}{dx}\left[(1+\bar{m})\,c_i\right] = \dot{s}_i + (1+\bar{m})\,\frac{w_i\, r^*}{\rho V} \qquad (1)$$

mass $$\frac{d}{dx}(1+\bar{m}) = \dot{m}$$

momentum $$\frac{d}{dx}\left[(1+\bar{m})\,V\right] = \dot{M} - \frac{(1+\bar{m})}{\rho V}\,\frac{dP}{dx} \qquad (3)$$

energy $$\frac{d}{dx}\left[(1+\bar{m})h_T\right] = \dot{H} \quad , \quad h_T = \sum_{i=1}^{n} c_i\, h_i + \frac{V^2}{2} \qquad (4)$$

*The independent variable, x, is taken as unitless with r* as the conversion factor to units. The quantity $1 + \bar{m}$ represents the streamtube mass flux normalized by the initial streamtube mass flux, i.e., $1 + \bar{m} = (\rho Va)/(\rho Va)_o$

if the expansion process is specified by the pressure distribution as a function of distance. Equations (1-4) can be written as

$$\frac{dc_i}{dx} = \frac{s_i - \dot{m}c_i}{1 + \bar{m}} + \frac{\dot{w}_i r^*}{\rho V} \tag{5}$$

$$\frac{dV}{dx} = \frac{\dot{M} - \dot{m}V}{1 + \bar{m}} - \frac{1}{\rho V}\frac{dP}{dx} \tag{6}$$

$$\frac{dT}{dx} = \frac{1}{C_P}\left[\frac{\dot{H} - \dot{m}\,h_T}{1 + \bar{m}} - \frac{V(\dot{M} - \dot{m}V)}{1 + \bar{m}} + \frac{1}{\rho}\frac{dP}{dx} - \sum_{i=1}^{n} h_i \frac{dc_i}{dx}\right] \tag{7}$$

$$\frac{d\rho}{dx} = \left[\frac{1}{P}\frac{dP}{dx} - \frac{1}{T}\frac{dT}{dx} - \frac{1}{R}\left(\sum_{i=1}^{n} R_i \frac{dc_i}{dx}\right)\right]\rho \tag{8}$$

where

$$C_p = \sum_{i=1}^{n} c_i C_{pi}, \quad \gamma = \frac{C_p}{(C_p - R)} \tag{9,10}$$

$$h_i = \int_0^T C_{pi}dT + h_{i0} \tag{11}$$

For each component of the gas, the equation of state is

$$P_i = \rho_i R_i T \tag{12}$$

Summing over all the components of the mixture, the over-all equation of state is obtained

$$P = \rho RT = \rho T \sum_{i=1}^{n} c_i R_i \tag{13}$$

The net species production rate $\omega_i$ for each species (component) is calculated from

$$\omega_i = \bar{m}_i \rho^2 \sum_{j=1}^{n} (\nu'_{ij} - \nu_{ij})\, X_j \tag{14}$$

where

$$X_j = \left[K_j \prod_{i=1}^{n} c_i^{\nu_{ij}} - \rho^{\lambda} \prod_{i=1}^{n} c_i^{\nu'_{ij}}\right] k_j \; M_j \tag{15}$$

Where $\lambda$ depends on the order of the reaction and $M_j$ is calculated only for dissociation-recombination reactions.

The equilibrium constant, $K_j$, is

$$K_j = e^{-\Delta F/\mathcal{R}T}, \qquad \Delta F = \sum_{i=1}^{n} f_i \nu_{ij} - \sum_{i=1}^{n} f_i \nu'_{ij} \tag{16}$$

The computer program considers chemical reactions defined by the generalized chemical reaction equation

$$\sum_{i=1}^{n} \nu_{ij} \bar{M}_i \rightleftarrows \sum_{i=1}^{n} \nu'_{ij} \bar{M}_i \tag{17}$$

where $\nu_{ij}$ and $\nu'_{ij}$ are the stoichiometric coefficients to be used in equation (15) while $\bar{M}_i$ represents the symbol for the $i^{th}$ chemical species.

The reaction rates, $k_j$, for the $j^{th}$ reaction appearing in equation (15) are represented in the Arrhenius form

$$k_j = a_j T^{-n_j} e^{(-b_j/\Re T)} \tag{18}$$

where

$a_j$ is the pre-exponential coefficient

$n_j$ is temperature dependence of the pre-exponential factor

$b_j$ is the activation energy

Since each dissociation-recombination reaction has a distinct reaction rate associated with each third body, the net production rate for each dissociation-recombination reaction should be calculated from

$$X_j = \sum_{k=1}^{n} \left[ K_j \prod_{i=1}^{n} c_i^{\nu_{ij}} - \rho \prod_{i=1}^{n} c_i^{\nu'_{ij}} \right] c_k k_{kj} \tag{19}$$

rather than equation (15). However, Benson and Fueno[6] have shown theoretically that the temperature dependence of recombination rates is approximately independent of the third body. Assuming that the temperature dependency of recombination rates is independent of the third body, the recombination rate associated with the $k^{th}$ species (third body) can be represented as

$$k_{kj} = a_{kj} T^{-n_j} e^{-b_j/\Re T} \tag{20}$$

where only the constants $a_{kj}$ are different for different species (third bodies). From equation (19) it can be shown that

$$X_j = \left[ K_j \prod_{i=1}^{n} c_i^{\nu_{ij}} - \rho \prod_{i=1}^{n} c_i^{\nu'_{ij}} \right] \left[ \sum_{i=1}^{n} \frac{a_{ij}}{a_{kj}} c_i \right] x \; a_{kj} T^{-n_j} e^{-b_j/\Re T} \tag{21}$$

Thus, the recombination rates associated with each third body can be considered as in equation (15) by calculating the general third body term $M_j$ as

$$M_j = \sum_{i=1}^{n} m_{ji} c_i \qquad (22)$$

where $m_{ji}$ is the ratio $a_{ij}/a_{kj}$.

In order to numerically integrate the above equations (1, 5, 6, 7) it is necessary to input the following type of information concerning the chemical system:

Boundary Conditions:

| | |
|---|---|
| $x_o$ | initial axial position |
| $P_o$ | initial pressure |
| $T_o$ | initial temperature |
| $V_o$ | initial velocity |
| $x_{max}$ | final axial position |
| $P(x)$ | table of pressure vs axial position |
| $dP(x)/dx$ | table of pressure derivatives vs axial position |

Species Information*:

| | |
|---|---|
| $\bar{M}_i$ | species name |
| $\bar{m}_i$ | species molecular weight |
| $C_{pi}(T)$ | species specific heat |
| $h_i(T)$ | species enthalpy |
| $f_i(T)$ | species free energy |

*The items $C_{pi}$, $h_i$, and $f_i$ are not available directly in the appropriate units. The computer program calculates these items for each species from the JANAF data for:

$C_p$ vs T

$H^\circ - H^\circ_{298}$ vs T

$-\frac{F^\circ - H^\circ_{298}}{T}$ vs T

and

$\Delta H^\circ_{f_{298}}$

Reaction Information:

| | |
|---|---|
| $\sum_{i=1}^{n} \nu_{ij} \bar{M}_i \rightleftarrows \sum_{i=1}^{n} \nu'_{ij} \bar{M}'_i$ | each reaction must be input in terms of its stoichiometric coefficients and constituent species |
| $a_j, n_j, b_j$ | constants defining $k_j$, the reaction rates |
| $m_{ji}$ | third body reaction-rate ratios |

Miscellaneous Information:

| | |
|---|---|
| $r^*$ | normalization factor for x |

Mass, Momentum, Energy, and Species Addition Functions:

| | |
|---|---|
| $\dot{m}(x)$ | mass addition rate, per unit normalized length, per unit initial streamtube mass flux |
| $\dot{M}(x)$ | momentum flux, per unit normalized length per unit initial streamtube mass flux |
| $\dot{H}(x)$ | energy addition rate, per unit normalized length, per unit initial streamtube mass flux |
| $\dot{s}_i(x)$ | $i^{th}$ species mass addition rate, per unit normalized length, per unit initial streamtube mass flux |

A considerable amount of data (such as JANAF tables defining $C_{pi}, h_i$, and $f_i$, reaction rate parameters and cards defining chemical reactions) are available with the computer program. Details concerning input to the computer program are given in Section 6.

## NUMERICAL METHOD

It has been shown (e.g. reference 3) that explicit methods of numerical integration are unstable when applied to relaxation equations (such as equations (1), (5), (6), (7)) unless the integration step size is of the order of the characteristic relaxation distance. Since in the near equilibrium flow regime the characteristic relaxation distance is typically many orders of magnitude smaller than characteristic physical dimensions of the system of interest, the use of explicit methods to integrate relaxation equations often results in excessively long computation times. An implicit integration method which is inherently stable in all flow situations (whether near equilibrium or frozen) is therefore used by the computer program. With this method step sizes which are of the order of the physical dimensions of the system of interest can be used, reducing the computation time per case several orders of magnitude when compared with conventional explicit integration methods.

Consider N first order simultaneous differential equations

$$\frac{dy_i}{dx} = f_i\,(x,\ y_1\ ,\ \ldots\ ,\ y_N) \qquad i = 1,\ 2,\ \ldots,\ N \tag{22}$$

with known partial derivatives (i.e. the Jacobian for the system)*

$$\alpha_i = \frac{\partial f_i}{\partial x} \tag{23}$$

$$\beta_{i,j} = \frac{\partial f_i}{\partial y_j} \tag{24}$$

The following implicit difference equations are used by the computer program to determine the $y_{i,n+1}$, (the subscript n denotes the $n^{th}$ integration step)

$$y_{i,n+1} = y_{i,n} + k_{i,n+1} \qquad ,h = x_{n+1} - x_n \tag{25}$$

where

$$k_{i,n+1} = \left[\ f_{i,n} + \alpha_{i,n} h + \sum_{j=1}^{N} \beta_{i,j,n} k_{j,n+1}\ \right] \cdot h \tag{26}$$

for the initial step and for restart (1st order).

*The computer program uses analytic expressions for calculation of the partial derivatives, $\alpha_i$, $\beta_{ij}$.

$$k_{i,n+1} = \frac{1}{3}\left[k_{i,n} + 2\left(f_{i,n} + \alpha_{i,n}h + \sum_{j=1}^{N} \beta_{i,j,n}k_{j,n+1}\right)\cdot h\right] \qquad (27)$$

for equal steps (2nd order with h = previous h)

$$k_{i,n+1} = \frac{h_{n+1}^2}{(2h_{n+1}+h_n)\cdot h_n}\left[ k_{i,n} + \left[f_{i,n}+\alpha_{i,n}h_{n+1} + \sum_{j=1}^{N} \beta_{i,j,n}k_{j,n+1}\right] \cdot \frac{h_n}{h_{n+1}}(h_{n+1}+h_n)\right] \qquad (28)$$

for unequal steps (2nd order with h ≠ previous h)

A derivation of these equations is given in reference 2.

If the flow is frozen, the explicit form of the above equations can be used ($\alpha_i = 0$, $\beta_{ij} = 0$), i.e. equations (26), (27), and (28) are each reduced from an NXN system of linear simultaneous equations to N explicit equations (N = 3 + No. of species).

Control of the integration step size, h, is provided by calculating estimates for the truncation error and comparing these to an input criterion, $\delta$.

The step size is halved if for any i = 1, 2, ...,N

$$E_i > \delta$$

The step size is doubled if for all i = 1, 2, ..., N

$$E_i < \frac{\delta}{10}$$

where

$$E_i = \left|\frac{k_{i,n+1} - 2k_{i,n} + k_{i,n-1}}{3k_{i,n+1} - k_{i,n}}\right|$$

The above expression for $E_i$ is derived in reference 2.

## 2. PROGRAM INPUT

This program was developed on the CDC 6400 computer using the FORTRAN IV language. The program uses CDC explicit overlay and requires a minimum of 35K core. Conversion to another computer system should be straight forward provided sufficient core storage is available. Program overlay extends three levels deep.

Input to the computer program is divided into the following 6 sections described below.

$THERMØ-namelist input which controls the thermodynamic data input

THERMODYNAMIC DATA - (optional)

TITLE CARD - also serves for plot labels

SPECIES CARDS - species to be considered and their initial concentrations

REACTION CARDS - input of reactions and rate data

$PRØPEL - namelist input for a specific case

A card listing for a complete input for a sample case is given in Table 3 at the end of this section.

$THERMØ

Permits the generation of a master thermodynamic file or the use of a tape file previously generated master thermodynamic file.

| Variable | | Value | Description |
|---|---|---|---|
| NUCHEM | = | 1 | A master thermodynamic file will be generated for this case on tape unit 4. Species and thermodynamic data will be read from unit INTAPE (nominal=5, the input file) and a new thermodynamic file will be generated on unit 4. The new thermodynamic file will be end-filed and rewound after generation. |
| | = | 0 | A previously generated master thermodynamic file will be used for this case. The master thermodynamic file must be file TAPE4. No other input variables are required for this option. |
| MAXSP | = | Input | If a master thermodynamic file is to be generated this variable specifies the the number of species for the master file. |
| LIST | = | 1 | A list of species names for those species master file will be output. |
| | = | 0 | This output will be deleted. |
| LISTX | = | 1 | Thermodynamic functions (CP, H, F) will be output for each species (one page per species, 52 lines per page). Species names, molecular weights and heats of formation will also be printed. |
| | = | -1 | Only a table of species names, molecular weights and heats of formation will be printed. |
| | = | 0 | The above output will be deleted. |
| INTAPE | = | Input | Tape file from which thermodynamic data is to be read (nominal = 5). |

$END

## THERMODYNAMIC DATA

For a NUCHEM = 1 option in $THERMØ the program will read MAXSP Master Species cards containing: species symbolic identifier, molecular weight, and $\Delta H^{\circ}_{F_{298}}$, and then read MAXSP sets of thermodynamic data (CP, H, F) checking names and card sequences. The Master Species cards must be sequenced sequentially in columns 41-50 (I10 format) and must correspond directly to the order in which the thermodynamic data is to be read. Thermodynamic functions consist of 10 cards per function, 5 values per card corresponding to temperature values of 100 → 5000°K at 100°K intervals. Table 1 lists the species for which thermodynamic data is currently available. For species which do not appear in Table 1 this input may be obtained directly from the JANAF tables. Table 2 is a sample listing of the thermodynamic function input for the species $N_2$.

Master Species Cards

| Col | Information |
|---|---|
| 1-10 | Not used |
| 11-16 | Species Symbolic Identifier, 6 alphanumeric characters (left justified) |
| 17-20 | Not used |
| 21-30 | Species Molecular weight (F) format |
| 31-40 | Species $\Delta H^{\circ}_{F_{298}}$ (F) format, K cals/mole |
| 41-50 | Right justified sequence number used for sequence checking on input (I10 format). |
| 51-80 | Not used |

It should be noted that a species is identified by the name assigned by the user. In general this name is the chemical symbol e.g. $O, O_2, H, H_2$. However, it may be useful to define a dummy species with all the properties of another species but which may be treated in a special manner, e.g. the percentage of the total amount of a species which is designated as an inert (possibly to simulate incomplete mixing or combustion). This may be done by defining species O and OX where OX is identical to O except in name, but does not appear in any reaction.

## Master Thermodynamic Function Cards

| Col | Information |
|---|---|
| 1 | Not used |
| 2-10 | Function Value at (100+500 (n-1)) °K, n= card number |
| 11 | Not used |
| 12-20 | Function Value at (200+500 (n-1)) °K |
| 21 | Not used |
| 22-30 | Function Value at (300+500 (n-1)) °K |
| 31 | Not used |
| 32-40 | Function Value at (400+500 (n-1)) °K |
| 41 | Not used |
| 42-50 | Function Value at (500+500 (n-1)) °K |
| 51-60 | Not used |
| 61-66 | Species Symbolic Identifier, left justified |
| 67-68 | Not used |
| 69-70 | Function Definition CP, H, or F, left justified |
| 73-76 | The word CARD |
| 77-78 | Card number 1-10 right justified |
| 79-80 | Not used |

Species Symbolic Identifier, Function Definition, and Card Numbers are checked for consistency on input.

TITLE CARD

The title card contains free field information which will be written as a header label for the program output. The first forty characters will be written as a label on each plot if plotting is requested.

SPECIES CARDS

This input is prefixed by a single card with SPECIES in columns 1 to 7 and with the words MASS FRACTIONS or MØLE FRACTIONS in columns 9-22. If the identifier for mass or mole fractions is omitted, mass fractions are assumed. Up to 40 species cards may be input. Only those species specified by input species cards will be considered. The order of the input species cards is independent of the order in which the species appear on the master thermodynamic data file. However, the order of the input species cards does define the species order for the specific calculation and other input referencing individual species must refer to the order of the input species cards. Species Cards are described below:

| Col | Function |
|---|---|
| 1-10 | Not used |
| 11-16 | Symbol (left justified) |
| 17-20 | Not used |
| 21-60 | Value of initial species concentration (if zero must be input as 0.0) free field F or E format |
| 61-80 | User Identification if desired |

Symbols For Species Identification

A chemical species is identified symbolically by 6 alphanumeric characters as follows:

The species symbol must agree with that given on its master species card (columns 11-16) used in generating the master thermodynamic file.

If the species is ionized, the degree of ionization is indicated by a + (or-) sign followed by an integer describing the degree of ionization (if no integer is given the species will be assumed singlely ionized.)

The species symbol may not contain the characters * or = . The special species symbol PHØTØN is reserved for specifying radiative reactions.

examples:

| Symbol | Interpretation |
|---|---|
| CL | $C\ell$ |
| NA+ | $Na^{+}$ |
| K+2 | $K^{++}$ |
| CL2-2 | $C\ell_2^{--}$ |
| H2O2 | $H_2O_2$ |

REACTION CARDS

This input is prefixed by a single card with REACTIONS in columns 1 to 9. Up to 50 dissociation reactions and a total 150 reactions may be input following this card. Only one card per reaction is permitted. Cards specifying dissociation-recombination reactions must precede cards specifying exchange reactions. The content and format of the reaction cards is defined as follows:

Each card is divided into five fields, separated by commas. Each field contains:

| | |
|---|---|
| field 1 | the reaction |
| field 2 | A= followed by the value of A |
| field 3 | N= followed by the value of N |
| field 4 | B= followed by the value of B, the activation energy (Kcal/mole) |
| field 5 | available for comments |

Rules for specifying the reaction are given below.

The values A, N, and B define the reverse reaction rate, k, as

$$k = A \cdot T^{-N} \cdot e^{-(B/RT)}$$

All three reaction rate parameters must be input. The numeric value of each parameter may be specified in either I, F, or E format. If E format is used the E must appear before the exponent.
There may be no blanks between the characters A and equal sign, the N and equal sign, and the B and equal sign.

Input rate parameters are in units of cc, °K, mole, sec.

The general form of a reaction is:

$$N_1 * \text{Symbol}_1 + N_2 * \text{Symbol}_2 + \ldots = N_a * \text{Symbol}_a + N_b * \text{Symbol}_b + \ldots$$

where the left hand side represents reactants and the right hand side represents products.

Each Symbol must be as defined on an input species card (see the description of SPECIES CARDS).

The multipliers, N, must be intergers and represent stoichiometric coefficients. If no stoichiometric coefficient is given, the value 1 is assumed. It is required that

$$N_1 + N_2 + .... \leq 10$$

and

$$N_a + N_b + .... \leq 10$$

examples:

| Reaction | Interpretation |
|---|---|
| NA++CL- = NACL | $Na^{+} + C\bar{l} = NaCl$ |
| B+2+M-2 = BM | $B^{++} + M^{--} = BM$ |
| BE+2+2*ØH- = BEØHØH | $Be^{++} + 2ØH^{-} = Be(ØH)_2$ |

The dissociation - recombination reactions specifying third body terms must precede other types of reactions, and must be followed by the directive:

Col 1 ↓

END TBR REAX

all reactions prior to the above directive will have a third body term added to each side of the reaction. E. g.

$H_2 = H + H, \ldots$

END TBR REAX

is the same as

$H_2 + M = H + H + M, \ldots$

where M is a generalized third body. Specific third body effects may be included by inputing specific third body reaction rate ratios XMM (J, I).

Radiative reactions may be considered using the special species PHØTØN. The PHØTØN may only appear on the left hand side of the equal sign for a reaction.

**The reaction set is terminated by a card containing LAST CARD in columns 1 to 9.**

$PROPEL

| Case Variables | | Units |
|---|---|---|
| Z | Initial normalized axial position | None |
| PI | Initial pressure | PSIA |
| T | Initial temperature | °R |
| V | Initial velocity | Ft/Sec |
| RSTAR | Axial distance normalizing factor | Inches |
| EXIT | Normalized axial distance for run termination | None |
| NOCHEM | = 1 if a frozen chemistry case is desired | None |

Plot Variables

| | | |
|---|---|---|
| IFP | = 1 | Plotting requested |
| ITP | = 1 | Plot temperature |
| IRØP | = 1 | Plot density |
| ICHEMP (1) | = | Species numbers for desired species concentration plots, up to 30 species |
| IXP | = 1 | Plot functions vs normalized distance |
| MLP | = 1 | Plot species MØLE fractions |
| MSP | = 1 | Plot species MASS fractions |

Print Variables

ND1 Print every ND3$^{rd}$ step beginning with the ND1$^{st}$ step until
ND2 the ND2$^{nd}$ step (The initial conditions and the EXIT point
ND3 are always printed)

Integration Variables

| | |
|---|---|
| HI | Initial normalized step size |
| HMIN | Minimum normalized step size |
| HMAX | Maximum normalized step size |
| DEL | Relative error criterion |
| JF | =0 all variables considered for step size control<br>=1 only fluid dynamic variables considered for step size control.<br>The variable which controls the step size, i.e. has the maximum relative error, is printed in the normal output under Integration Parameters, labeled Governing Equation. The number:variable correspondence is as follows: 1=T;2=RO; 3 = V; 4 = Species 1;5 = Species 2; . . . NSP + 3 = Species NSP. |

## Table Input Variables

| | | |
|---|---|---|
| NTB | | number of input table entries for pressure table ( 101) |
| JPFLAG | | Determines the type of differentiation used to obtain derivatives for all input tables. Reference should be made to Mass, Momentum, Energy and Species Addition Functions for other input tables controlled by JPFLAG. |
| | | = 1 derivatives of input table obtained by simple difference formulae with second derivatives defined as 0. |
| | | = 2 derivatives of input tables obtained by SPLINE fit (NTB ≤ 20) |
| | | = 3 derivatives input along with tables |
| | | = 4 derivatives of input tables obtained by parabolic differentiation (NTB ≤ 20) |
| PSCALE | = | Multiplicative constant for the input pressure table |
| ZTB (1) | = | Normalized axial positions for input tabular values for pressure table (always input) |
| PTB (1) | = | Pressure table (PSIA) (always input) |
| DPTB (1) | = | Pressure table derivative (for JPFLAG = 3 option). |

## Miscellaneous Variables

| | |
|---|---|
| XMM(J,I) | Reaction rate ratio effect on reaction J of species I |
| TU(1) | Temperature above which approximate extension of JANAF tables will occur for each species (nominal = 9000°R) |
| IFLAST | For overlay reasons must be set = 1 on the last case of a run |
| TSTØP | Time at which a run will arbitrarily be terminated (CP time) |

## Intermediate Output

| | | |
|---|---|---|
| IDQDX | = 1 | Print total derivatives |
| IDXJDX | = 1 | Print individual reaction net production rates |
| IEQØUT | = 1 | Print equilibrium constant and its temperature dependence in internal units |
| IRATE | = 1 | Print reaction forward and reverse rates in internal units |
| IMASDX | = 1 | For an IADDF = 1 option print chemical and addition function components of total derivatives |
| IØPXF | = 1 | Print influence coefficient vectors |
| IØPVAR(1) | = | Set consecutive entries equal to K for variables for which influence coefficient vectors are to be output, where |

| K | Variable |
|---|---|
| 1 | V |
| 2 | RØ |
| 3 | T |
| 4 | Species No. 1 |
| . | . |
| . | . |
| . | . |
| . | . |
| NSP+3 | Species No. NSP |

For example: IØPVAR(1) = 4,3, will output influence coefficient vectors for species number 1 and for temperature.

Mass, Momentum, Energy, and Species Addition Functions

| Variable | | |
|---|---|---|
| IADDF | = 1 | Addition functions will be input |
| IXTB | = | Number of entries in addition function tables 40 |
| IADDØP | = 0 | Addition functions input via tables |
| | = 1 | Addition functions defined via multiplicative factors See EFACT (I), XMFACT (I), SPFACT (I, J) below. Note that IXTB factors must be input. |
| | = 2 | A subroutine for addition calculation will be supplied by the user |
| XADSCL | = | Multiplicative scale factor for all addition functions Note that input of XADSCL as 1.0/( .V.A) will provide automatic normalization (per unit initial streamtube mass flux) for input addition functions. |
| ADDX (I) | = | Table of normalized axial stations for all input addition functions |
| ADDMAS (I) | = | Mass addition rate, per unit normalized length, per unit initial streamtube mass flux (unitless) |
| ADDE (I) | = | Energy addition rate, per unit normalized length, per unit initial streamtube mass flux (BTU/lb) |
| ADDEX (I) | = | Auxillary energy addition rate, per unit normalized length, per unit initial streamtube mass flux (BTU/lb) which will be added to the energy addition rate ADDE (I). Note that ADDEX (I) is independent of EFACT (I) for IADDØP = 1 option and will be added to ADDE (I) before modification by XADSCL |
| ADDMØM (I) | = | Momentum flux, per unit normalized length, per unit initial streamtube mass flux (ft/sec) |
| NPOINT (I) | = | Species number (for current case) to relate species addition functions to specific species. See example under ADDSP (I, J). |
| NSPADD | = | Number of entries in NPØINT (I) table |
| ADDSP (I, J) | = | Species mass addition rate per unit normalized length, per unit initial streamtube mass flux (unitless) |

I=1,. . . IXTB corresponding to number of entries

J=1,. . . NSPADD

e.g., NSPADD = 2

NPØINT = 3, 5

ADDSP (I, 1) corresponds to Species 3

ADDSP (I, 2) corresponds to Species 5

| | | |
|---|---|---|
| EFACT (I) | = | For IADDOP = 1, ADDE (I) computed as ADDMAS(O)*EFACT(I) |
| XMFACT (I) | = | For IADDØP = 1, ADDMØM (I) computed as ADDMAS (I) *XMFACT (I) |
| SPFACT (I, J) | = | For IADDØP = 1, ADDSP (I, J) computed as ADDMAS (I) *SPFACT (I, J) |
| IHTØTF | = 1 | Restart flag indicating that a case is being restarted and directing the initial enthalpy to be HTØTX |
| HTØTX | = | Initial enthalpy if a case has been restarted ($ft^2/sec^2$) |
| DMASDX (I) | = | For JPFLAG = 3 option, derivative of the mass addition rate $d(ADDMAS)/d\bar{x}$ |
| DEDXT (I) | = | For JPFLAG = 3 option, derivative of the total energy addition rate $d(ADDE+ADDEX)/d\bar{x}$ |
| DMØMDX (I) | = | For JPFLAG = 3 option, derivative of the momentum addition rate $d(ADDMØM)/d\bar{x}$ |
| DSPDX (I, J) | = | For JPFLAG = 3 option, derivative of the species addition rate $d(ADDSP)/d\bar{x}$ |

## Generalized Oblique Shock Calculation

A generalized oblique shock calculation is specified by input of a pressure table containing a pressure discontinuity, and a pointer designating the shock location.

| | | | UNITS |
|---|---|---|---|
| NSHØCK | = | Pointer designating the last entry in the pressure table prior to the shock<br>e.g. $\frac{P_2}{P_1} = \frac{PTB(NSHOCK+1)}{PTB(NSHOCK)}$<br>Entries NSHOCK and NSHOCK+1 in the pressure table must have the same axial position. | None |
| SHKBUG | = | 1.0 provides intermediate output<br>0.0 provides no intermediate output | None |
| SMAXIT | = | Maximum number of iterations during a generalized oblique shock calculation | None |
| SKEPS(1) | = | Relative convergence criterion for temperature iteration during a generalized oblique shock calculation | None |
| SKEPS(2) | = | Relative convergence criterion for overall iteration during a generalized oblique shock calculation | None |

## Normal Shock Stagnation Streamline Calculation

The normal shock stagnation streamline calculation option performs a normal shock calculation from specified upstream and downstream velocities and continues the calculation as a velocity defined streamtube.

| | | | UNITS |
|---|---|---|---|
| NSTAGV | = | 1 specifies a normal shock stagnation streamline calculation | none |
| VEL1 | = | Upstream velocity for the normal shock calculation | ft/sec |
| VTB(1) | = | Array defining the velocity as a function of normalized axial distance. VTB(1) is defined as the downstream velocity for the normal shock calculation | ft/sec |
| NVTB | = | Number of entries in the velocity profile NVTB ≤ 101 | none |

Reaction Screening Input Variables

If a reaction screening calculation is requested, the program performs a two pass calculation. The first pass utilizes the complete reaction set and determines those reactions which must be retained to satisfy the input criteria for each species screened. The second pass redoes the first calculation with an edited reaction set and provides a summary page comparing both calculations.

| | | | UNITS |
|---|---|---|---|
| ISCRF | = | 1, specifies a reaction screening case for ISCSP (1) species | none |
| ISCSP(1) | = | Species number for those species to be screened ≤ 40 | none |
| EPSCR(1) | = | Relative retention criterion for each species to be screened. Defined as the maximum change in mass fraction relative to production or destruction of the species per unit normalized length for all reactions involving the corresponding species. ≤ 40 | none |
| ISCBUG | = | 1 provides intermediate output during the reaction screening procedure. | none |

TABLE 1

SPECIES RESIDING ON MASTER THERMODYNAMIC TAPE

| | | | | | |
|---|---|---|---|---|---|
| 1 H2O | 19 SF4 | 37 BCL3 | 55 C2F2 | 73 COF2 | 90 ALF |
| 2 H2 | 20 SF6 | 38 BF | 56 O3 | 74 NO3 | 91 ALF2 |
| 3 OH | 21 C | 39 BF2 | 57 HO2 | 75 NH | 92 ALF3 |
| 4 O2 | 22 CO2 | 40 BF3 | 58 NO2- | 76 NH2 | 93 ALOCL |
| 5 O | 23 CO | 41 BOCL | 59 NA | 77 NH3 | 94 ALOF |
| 6 H | 24 C2 | 42 BOF | 60 NA+ | 78 BH | 95 ALCLF |
| 7 ARGON | 25 CH | 43 BCLF | 61 NAO | 79 BH2 | 96 ALCL2F |
| 8 F2 | 26 CH2 | 44 BCL2F | 62 CF2 | 80 BH3 | 97 ALCLF2 |
| 9 HF | 27 CH3 | 45 BCLF2 | 63 CF3 | 81 B2H6 | 98 OH- |
| 10 F | 28 CH4 | 46 B | 64 CF4 | 82 B2O2 | 99 CH2O |
| 11 N2 | 29 C2H2 | 47 CL | 65 C2F4 | 83 B2O3 | 100 NAOH |
| 12 NO | 30 CN | 48 CL2 | 66 NO2 | 84 AL | 101 NAH |
| 13 NO+ | 31 HCN | 49 N | 67 N2O | 85 ALO | 102 F22 |
| 14 O2- | 32 BN | 50 HCL | 68 HCO | 86 AL2O | 103 F2 |
| 15 O- | 33 BO | 51 CLF | 69 HCO+ | 87 ALCL | 104 OHX |
| 16 F- | 34 BO2 | 52 CNCL | 70 C2H | 88 ALCL2 | 105 PHOTON |
| 17 F- | 35 BCL | 53 CNF | 71 H3O+ | 89 ALCL3 | 106 O2 |
| 18 S | 36 BCL2 | 54 CF | 72 H2O2 | | |

TABLE 2

SAMPLE LISTING FOR THERMODYNAMIC FUNCTION CARDS
FOR N2

```
 6,9560,   6,9570,   6,9610,   6,9900,   7,0690,   N2  CP  CARD 1
 7,1960,   7,3500,   7,5120,   7,6700,   7,8150,   N2  CP  CARD 2
 7,9450,   8,0610,   8,1620,   8,2520,   8,3300,   N2  CP  CARD 3
 8,3980,   8,4580,   8,5120,   8,5590,   8,6010,   N2  CP  CARD 4
 8,6380,   8,6720,   8,7030,   8,7310,   8,7560,   N2  CP  CARD 5
 8,7790,   8,8000,   8,8200,   8,8380,   8,8550,   N2  CP  CARD 6
 8,8710,   8,8860,   8,9000,   8,9140,   8,9270,   N2  CP  CARD 7
 8,9390,   8,9500,   8,9620,   8,9720,   8,9830,   N2  CP  CARD 8
 8,9930,   9,0020,   9,0120,   9,0210,   9,0300,   N2  CP  CARD 9
 9,0390,   9,0480,   9,0570,   9,0660,   9,0740,   N2  CP  CARD10
-1,3790,   -,6830,    ,0130,    ,7100,   1,4130,   N2  H   CARD 1
 2,1250,   2,8530,   3,5960,   4,3550,   5,1290,   N2  H   CARD 2
 5,9170,   6,7180,   7,5290,   8,3500,   9,1790,   N2  H   CARD 3
10,0150,  10,8590,  11,7070,  12,5600,  13,4180,   N2  H   CARD 4
14,2800,  15,1460,  16,0150,  16,8860,  17,7610,   N2  H   CARD 5
18,6380,  19,5170,  20,3980,  21,2800,  22,1650,   N2  H   CARD 6
23,0510,  23,9390,  24,8290,  25,7190,  26,6110,   N2  H   CARD 7
27,5050,  28,3990,  29,2950,  30,1910,  31,0890,   N2  H   CARD 8
31,9880,  32,8880,  33,7880,  34,6900,  35,5930,   N2  H   CARD 9
36,4960,  37,4000,  38,3060,  39,2120,  40,1190,   N2  H   CARD10
51,9570,  46,4070,  45,7700,  46,0430,  46,5610,   N2  F   CARD 1
47,1430,  47,7310,  48,3030,  48,8530,  49,3780,   N2  F   CARD 2
49,8790,  50,3570,  50,8130,  51,2480,  51,6650,   N2  F   CARD 3
52,0650,  52,4480,  52,8160,  53,1710,  53,5130,   N2  F   CARD 4
53,8420,  54,1600,  54,4680,  54,7660,  55,0550,   N2  F   CARD 5
55,3350,  55,6060,  55,8700,  56,1270,  56,3760,   N2  F   CARD 6
56,6190,  56,8540,  57,0870,  57,3120,  57,5320,   N2  F   CARD 7
57,7470,  57,9570,  58,1620,  58,3620,  58,5590,   N2  F   CARD 8
58,7510,  58,9400,  59,1240,  59,3050,  59,4820,   N2  F   CARD 9
59,6570,  59,8270,  59,9950,  60,1600,  60,3220,   N2  F   CARD10
```

TABLE 3

CARD LISTING FOR A SAMPLE CASE

```
          H2          .01
          O2          .01
          ARGON       .98
          H2O         0.0
          O           0.0
          H           0.0
          O3          0.0
          OH          0.0
          OHX         0.0
          HO2         0.0
          H2O2        0.0
          PHOTON      0.0
REACTIONS
 H2       = H + H  ,    A=8.00E17,   N=1.0,    B=0.0,
 O2       = O + O  ,    A=1.90E16,   N=0.5 ,   B=0.0   ,
 H2O      = OH + H ,    A=1.17E17,   N=0.0,    B=0.0   ,   LEEDS 2 VQ
 HO2      = O2 + H ,    A=1.59E15,   N=0.0 ,   B=-1.0  ,   LEEDS 3
 OH       = O + H  ,    A=2.00E18,   N=1.0 ,   B=0.0   ,
 OH + OH = H2O2    ,    A=1.17E17,   N=0.0 ,   B=45.5  ,   LEEDS 3  Q
 OHX + PHOTON = O+ H,   A=1.00E14,   N=0.0,    B=0.0   ,
END TBR REAX
 H2O + H = H2 + OH ,    A=2.19E13,   N=0.0 ,   B=5.15  ,   LEEDS 2
 OH + H  = H2 + O  ,    A=1.74E13,   N=0.0,    B=9.45,     LEEDS 2
 OH + O  = O2 + H  ,    A=3.00E14,   N=0.0,    B=16.8,
 OH + OH = H2O + O ,    A=5.75E13,   N=0.0 ,   B=18.0  ,   LEEDS 2 VQ
 H2O + HO2 = H2O2 + OH, A=1.00E13,   N=0.0 ,   B=1.8   ,   LEEDS 3  H
  H2O2 + H = H2 + HO2,  A=9.60E12,   N=0.0 ,   B=24.0  ,   LEEDS 3R
 OH + PHOTON = OHX ,    A=1.8E6,     N=0.0,     B=0.0,
```

TABLE 3 (Continued)

```
$PROPEL
Z=0.0, PI=.735, T=527.4, V=4385.8, RSTAR=12.0, EXIT=.3,
ND3=5,
HI=.002, HMIN=.002, HMAX=0.2, DEL=0.001, JF=0,
NTB=4, JPFLAG=1, PSCALE=.7350,ZTB(1)=0.0, 0.01, 0.01, 100.0,
PTB(1)=1.0, 1.0, 22.1, 22.1,
TCOND(1)=40*0.0,
XMM=2000*1,
XMM(1,1)=5.0, XMM(1,4)=15.0,
XMM(3,1)=0.25, XMM(3,2)=0.25, XMM(3,3)=0.06,
XMM(4,1)=5.0, XMM(4,2)=2.0, XMM(4,4)=32.5,
IFLAST=1,
TSTOP=120.0
NSHOCK=2, SHKBUG=1.0,
ISCRF=1, ISCSP(1)=6, EPSCR(1)=.01,ISCBUG=1,
EXIT=0.3,
EXIT=.2,
$END
```

## REFERENCES


1. Kliegel, J.R. and Frey, H. M., "One-Dimensional Reacting Gas Nonequilibrium Performance Program," 02874-6003-R000, March, 1967, TRW Systems, Redondo Beach, Calif.

2. Kliegel, J R., Frey, H. M., Nickerson, G. R., and Tyson, T. J., "TCRPG One-Dimensional Kinetic Nozzle Analysis Computer Program," published by Dynamic Science, under contract NAS7-443, July 1968.

3. Tyson, T. J. and Kliegel, J. R., "An Implicit Integration Procedure for Chemical Kinetics," AIAA 6th Aerospace Sciences Meeting, Paper No. 68-180, January 1968.

4. Hirschfelder, J.O., Curtiss, C. F., and Bird, R. B., Molecular Theory of Gases and Liquids, Wiley, New York, 1954.

5. Penner, S. S., Chemistry Problems in Jet Propulsion, Pergamon New York, 1957.

6. Benson, S. W. and Fueno, T., "Mechanism of Atom Recombination by Consecutive Vibrational Deactivations," Journal of Chemical Physics, Vol. 36, 1962, pp 1597-1607.

# APPENDIX B

# EXPERIMENTAL EQUIPMENT

## APPENDIX B

### 1. GENERAL DESCRIPTION OF THE SHOCK TUBE FACILITY

The Dynamic Science shock tube consists of a driver section diaphragm holder, driven section, acceleration section and test section, supported on a 9 inch wide steel channel. An overall view of the facility is shown in Figures B-1 and B-2.

#### a. Driver

The driver has an internal diameter of 3.250 inches, a wall thickness of .500 inches, and a total length of 5 feet. It is constructed of type 304 stainless steel, the design operating pressure being 2500 psi with a safety factor of 5.

For ease of handling during diaphragm replacement the driver is mounted on roller supports.

#### b. Diaphragm Holder

The diaphragm holder is of the free piston design and is shown in Figure B-3. Any elongation of the clamping bolts due to the pressure load allows the piston to move and maintain the clamping load on the diaphragm.

To help prevent the diaphragm petals from rebounding and creating additional flow disturbances the internal surface of the downstream section of the diaphragm holder has been grooved permitting the petals to deform instead of bouncing. To further insure clean petalling without loss of diaphragm material, the diaphragms are scribed in the form of a $90^{\circ}$ cross by a milling machine with either $60^{\circ}$ or $90^{\circ}$ included angle cutters. A typical diaphragm before and after rupture is shown in Figure B-4.

#### c. Driven and Acceleration Sections

The 10 foot driven section and the acceleration section, composed of two 10 foot sections, are essentially identical in construction. Both have wall thicknesses of .500 inches and inside diameters of 3.250 inches with all internal surfaces honed to a 32 micro-inch finish to minimize wall viscous effects.

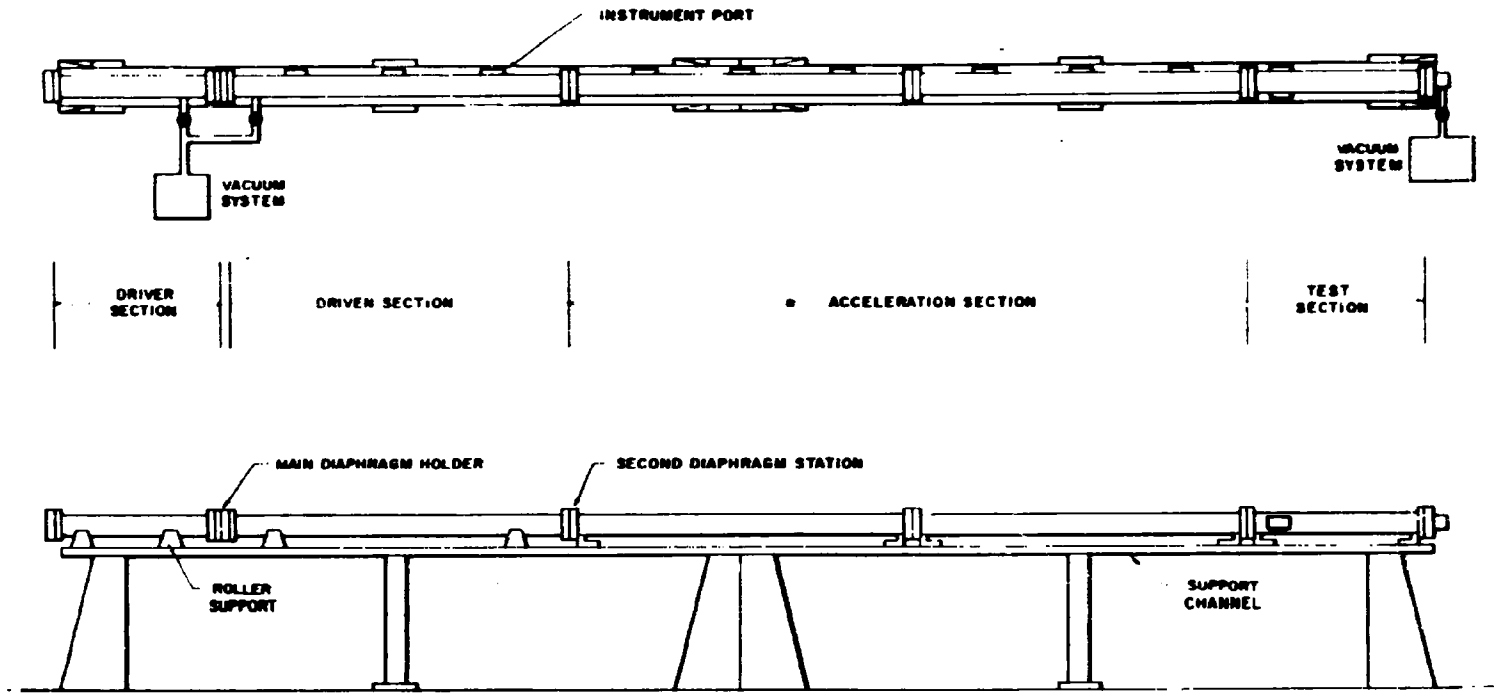


Figure B-1. Schematic Assembly.

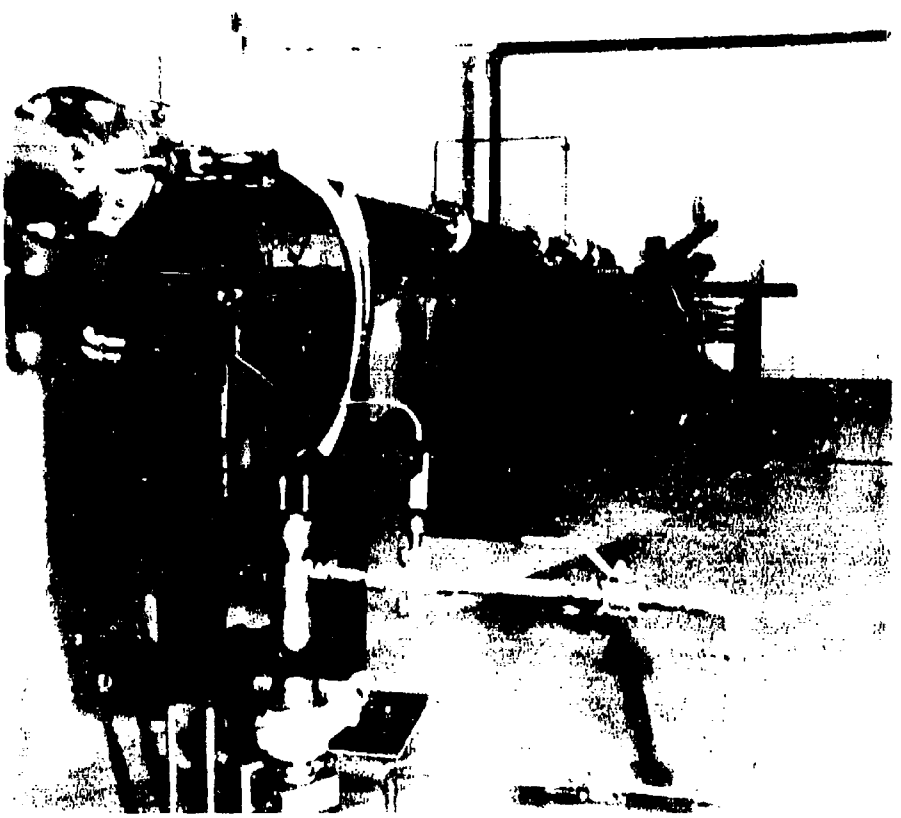

Figure B-2. Shock Tube

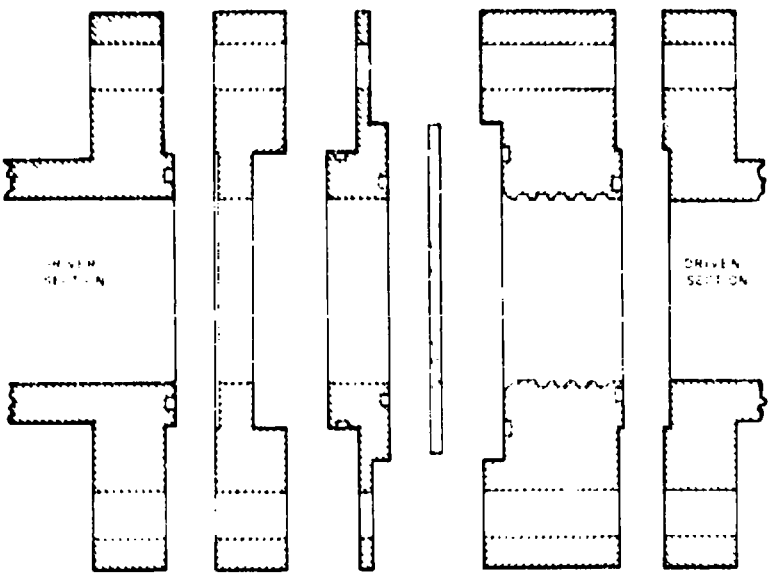

Figure B-3. Diaphragm Holder.

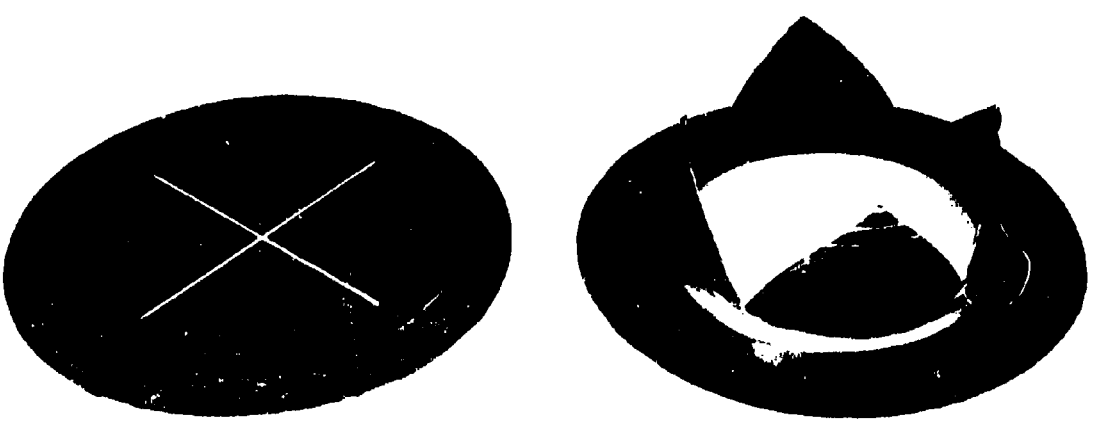

Figure B-4. Shock Tube Diaphragm.

Alignment of adjacent sections is maintained by utilizing spigot and counterbore joints. A port is provided in the end of the driven section nearest to the main diaphragm for evacuation and sample gas loading.

To permit access to the second diaphragm station the driven section is supported on roller mounts.

Each 10 foot section contains three equally spaced instrument ports which can accommodate either thin film heat transfer gauges for shock wave velocity measurements, or pressure transducers.

d. Test Section

The test section is an assembly of two components, a circular tube with a 6 inch internal diameter and a .375 inch wall thickness, and a mating rectangular insert. The rectangular insert (shown in Figure B-5) slides inside the circular tube with its wedge shaped leading edges protruding into the end of the acceleration section. The observation windows are mounted on the rectangular insert and are isolated from the flow eternal to the insert by the window clamps shown in Figure B-6.

The purpose of this assembly is to remove a rectangular gas sample from the cylindrical flow in the acceleration section and then isolate it from the remainder of the flow. The plane flow geometry obtained in this manner enables a simplified reduction of the experimental data.

A spring loaded piston relief valve is fitted into the end plate of the test section. In case of an unexpected overpressure this valve opens a one inch diameter port to atmosphere allowing the high pressure gas to be vented outside the building.

2. SHOCK TUBE OPERATION

a. Pressurization and Vacuum Systems

The shock tube pressurization and vacuum systems are shown schematically in Figure B-7. A 16 inch Bourdon type pressure gauge is used to measure the driver pressure during the pressurization process. A check valve in the line connecting the gauge to the driver section maintains the gauge at the pressure

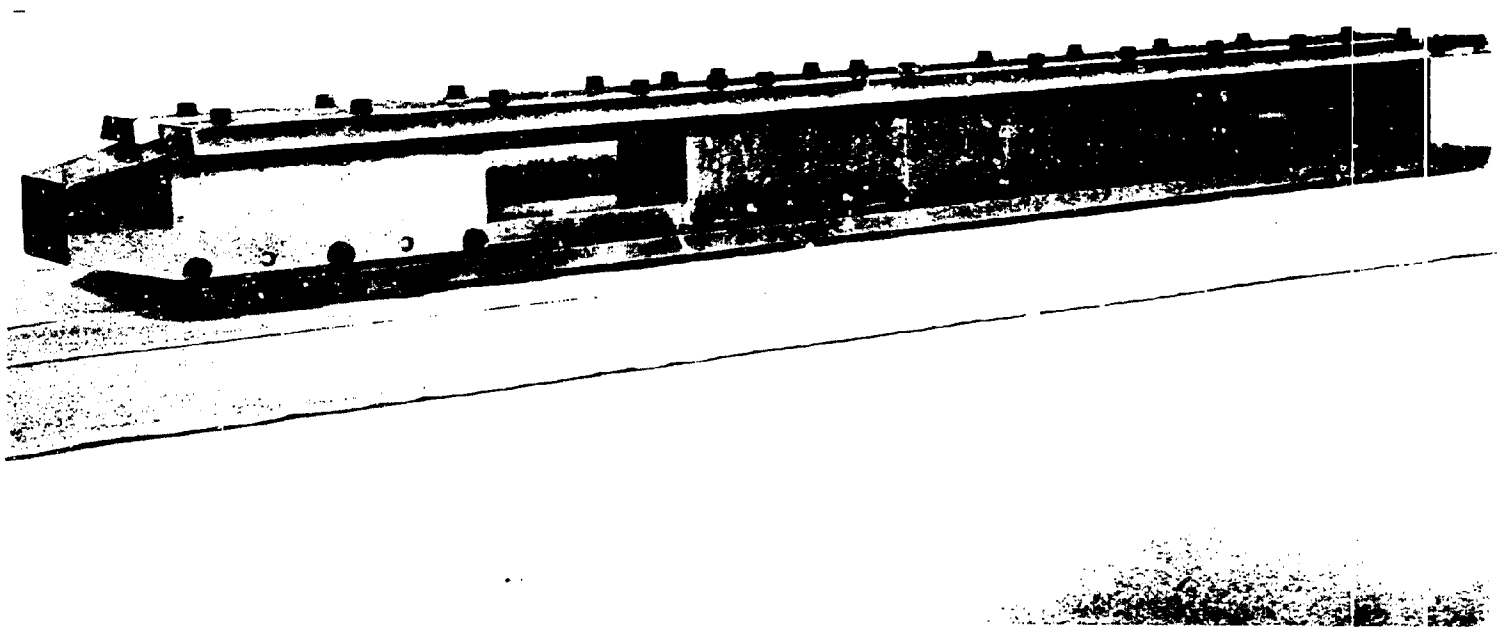

Figure B-5. Test Section Rectangular Insert.

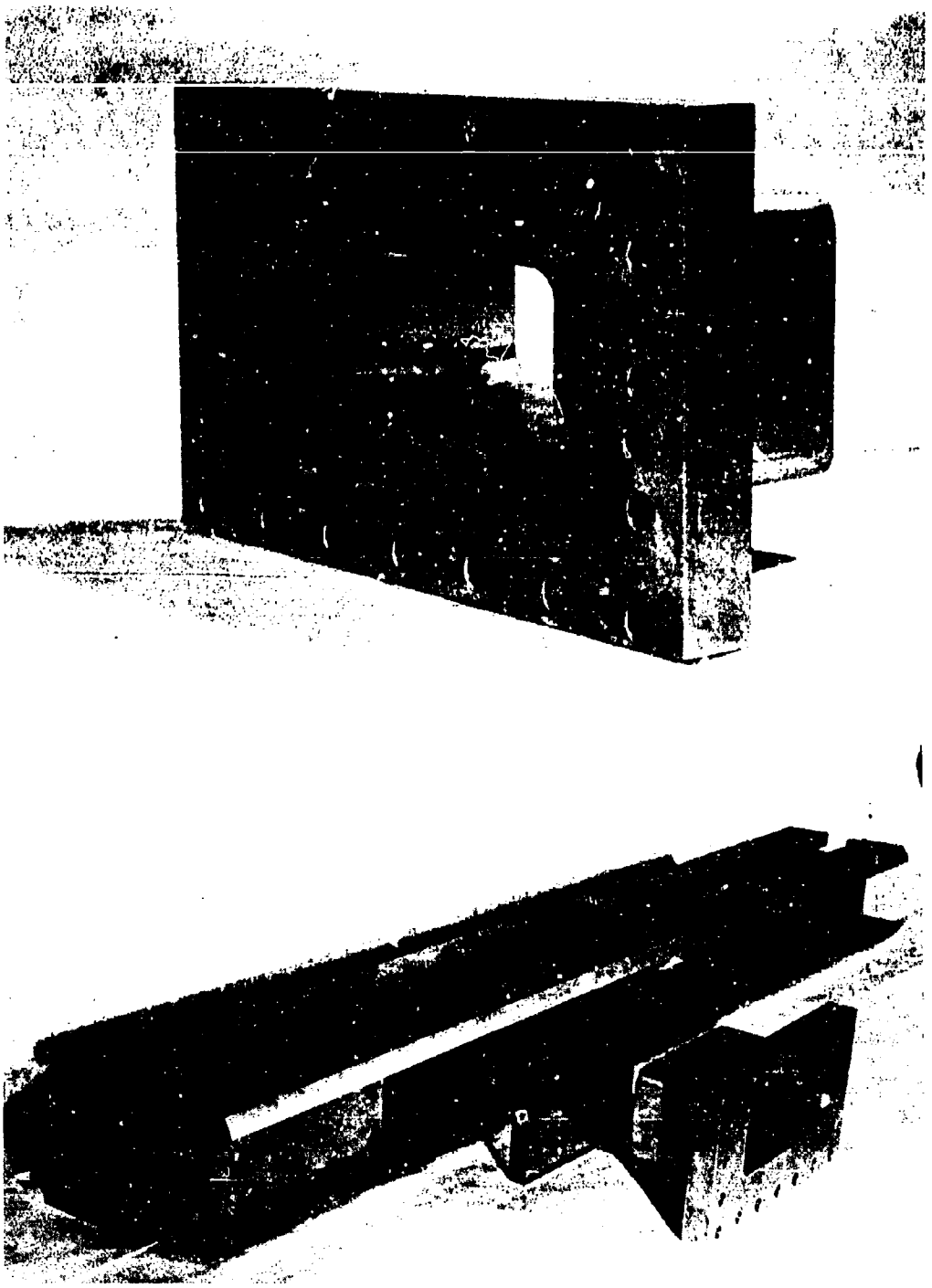

Figure B-6. Window Clamp and Assembly.

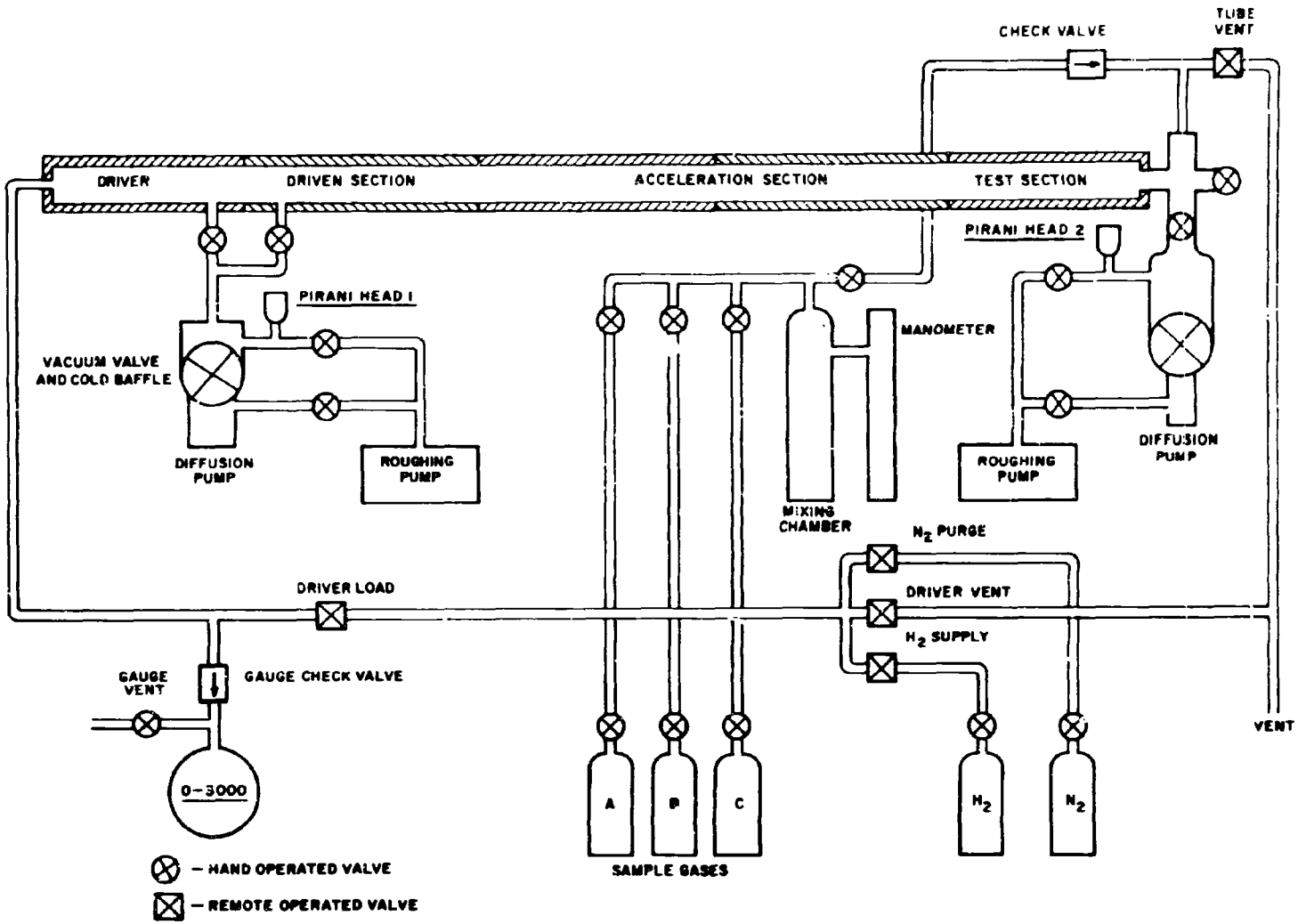


Figure B-7. Vacuum and Pressurization System Schematic.

reached at the time of diaphragm rupture. This permits a more accurate calibration of driver pressure versus diaphragm thickness and scribe depth.

Two vacuum systems composed of roughing pumps and 2 inch oil vapor diffusion pumps are used to evacuate the tube prior to the loading of the sample gas. One set of pumps evacuates the acceleration and test sections and the other evacuates the driver and driven sections. When evacuated, the tube pressure and leak rate are measured by Edwards High Vacuum Model M6A Pirani Gauge heads.

The controls operating the remote actuated valves, and the Pirani gauge head read out, are located in the console shown in Figure B-8.

The sample gas mixture is prepared by admitting the correct partial pressure of the individual components of the desired mixture into the mixing chamber. The partial pressures and the final total pressure are measured with a mercury manometer.

## 3. INSTRUMENTATION

### a. Shock Speed Measurement

The shock wave velocity is determined from the time required by the shock wave to pass thin film heat transfer gauges located at known intervals along the tube. Signals from these gauges are suitably amplified, pseudo-differentiated, and then displayed on a rastered sweep by a Tektronix type 556 oscilloscope. The rastered sweep is obtained from the method described in Reference B-1. A Tektronix type 184 Time Mark Generator is used to intensity modulate the sweep, providing an accurate time base for the measurement of the inter-signal time intervals.

The heat transfer gauges were constructed by bonding a thin film of platinum on 5 mm diameter pyrex rods, using Liquid Bright Platinum No. 05 (Hanovia Liquid Gold Division, Engelhard Industries), and following the procedures given in Reference B-2.

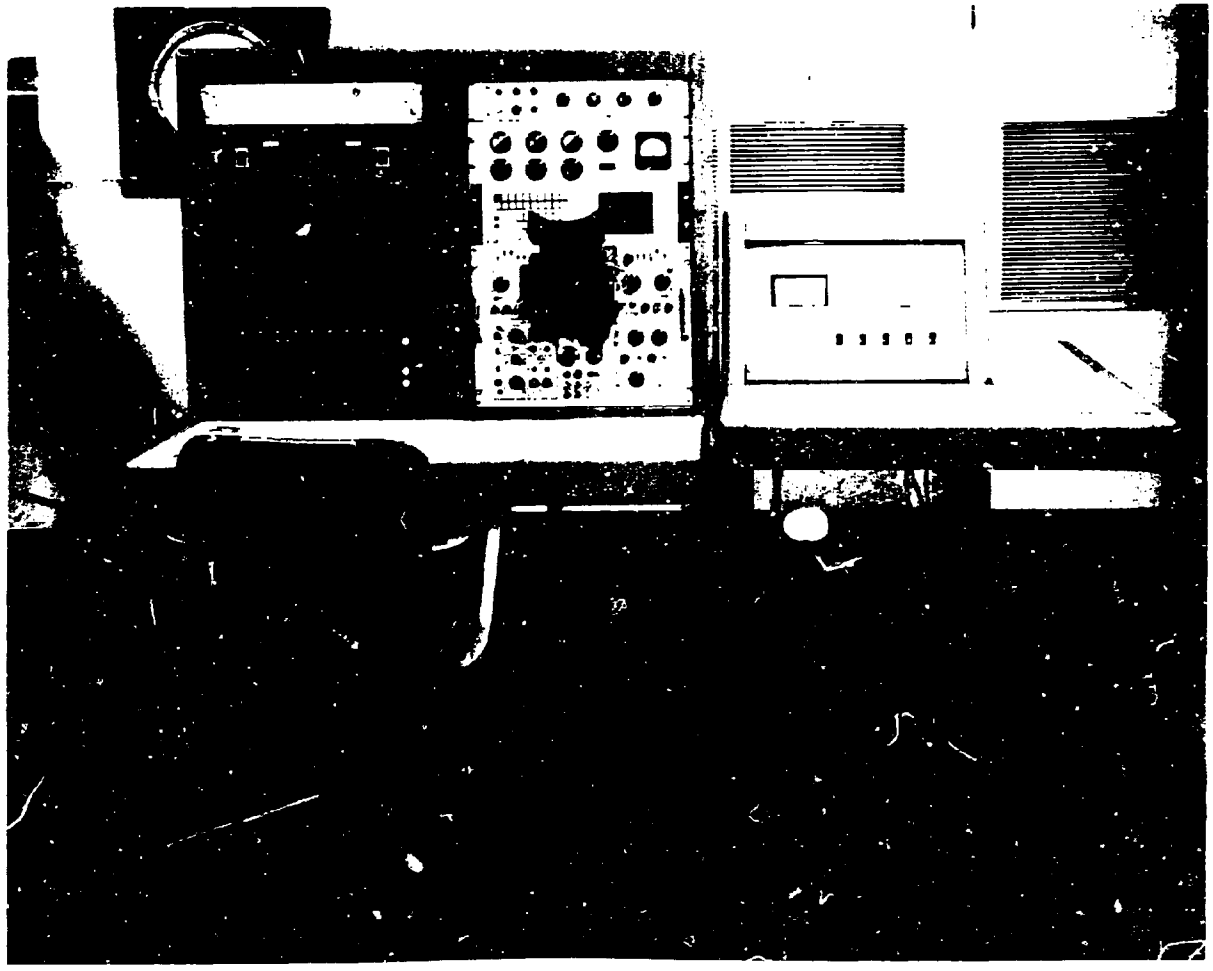

Figure B-8. Operating Console.

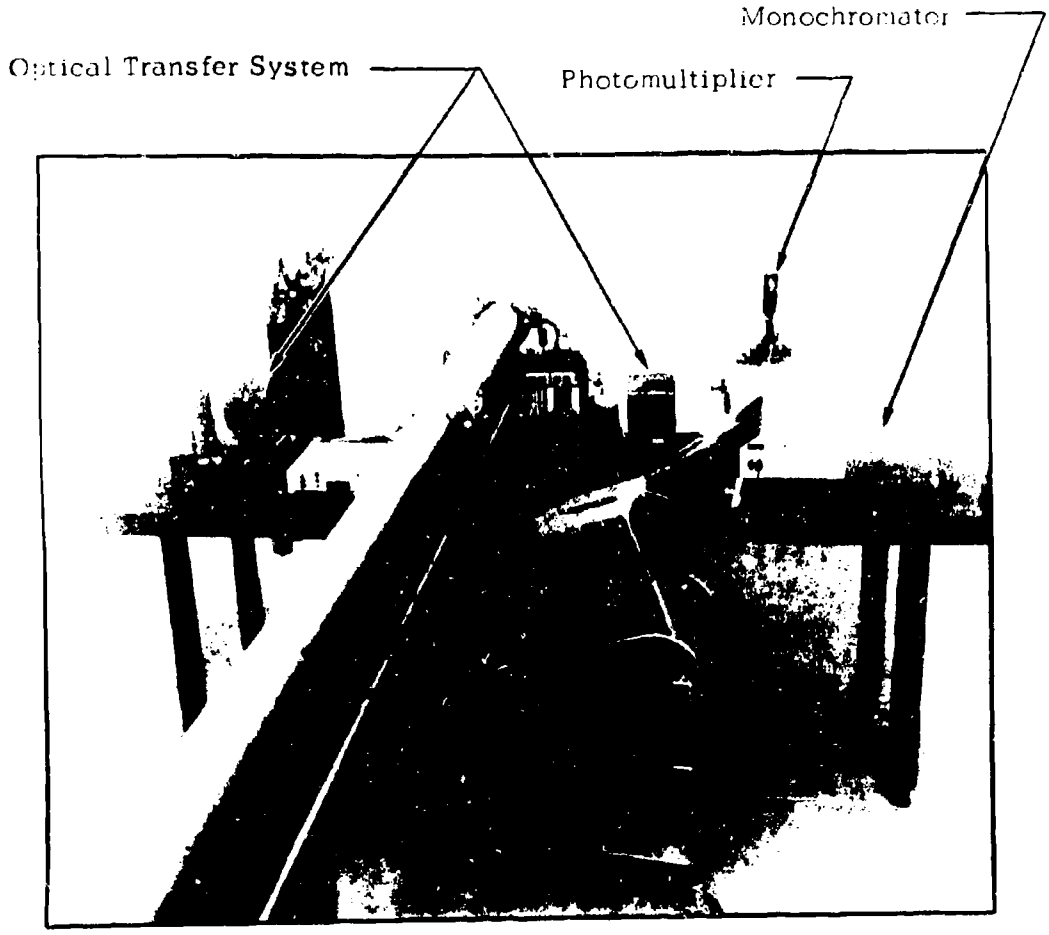


Figure B-9. Spectroscopic Instrumentation.

b. Spectroscopic Instruments

The analytical instruments currently in use with the shock tube have the capability of determining chemical specie concentrations by absorption or emission spectroscopy. The instrumentation (shown in Figure B-9) consists of a Warner and Swasey Model 21 Focused Radiation Source and Model 30 Optical Transfer System which illuminate the entrance slit of a Hilger-Engis Model 600 Monochromator-Spectrometer with radiation emanating from the test section of the shock tube. The Monochromator-Spectrometer is constructed so as to allow the intensity of several spectral lines with significantly different wave lengths to be monitored simultaneously by photomultiplier tubes. The photomultiplier used in the experiments discussed above is an EMI 9601B (S-11C photocathode) with the operating voltage supplied by a Sorenson power supply.

c. Monochromator Dispersion and Operating Bandwidth

The general equation which relates the dispersion angle at a given wavelength to the configuration of the instrument and the properties on the grating used is

$$s\lambda = \frac{1}{\beta} (\sin i + \sin \varphi) \qquad (1)$$

$s$ = the order used

$\beta$ = the number of rulings per $^{\circ}A$ on the grating

$i$ = angle of incidence

$\varphi$ = angle of diffraction

For this instrument

$$\varphi = w - \Phi$$

$$i = w + \Phi$$

Therefore, (1) becomes

$$s\lambda = \frac{2}{\beta} \sin w \cos \Phi \qquad w = \sin^{-1} \frac{s\lambda\beta}{2 \cos \Phi} \qquad (2)$$

The dispersion in °A per degree is found by differentiating (1)

$$\frac{d\lambda}{d\varphi} = \frac{\cos w}{\beta s}$$

Linear distance at the exit focal plane is related to the diffraction angle by

$$\ell = f \tan \varphi \qquad (3)$$

f = focal length of instrument

Differentiating (3) gives

$$\frac{d\varphi}{d\ell} = \frac{\cos^2 \varphi}{f}$$

Therefore, the dispersion at the exit focal plane in °A/mm is given by

$$\frac{d\lambda}{d\ell} = \frac{d\lambda}{d\varphi} = \frac{d\varphi}{d\ell}$$

$$\frac{d\lambda}{d\ell} = \frac{\cos w \cos^2 \varphi}{\beta sf}$$

when f is in units of mm.

For the present instrument

$$\frac{d\lambda}{d\ell} = 27.7 \text{ °A/mm}$$

at $\lambda = 3080$ °A.

Figure B-10 presents the measured intensity of the mercury 2967.3 °A line versus monochromator wavelength setting at 1 °A intervals. Using the calculated dispersion, the bandwidth of uniform intensity transmission is found to be 21.8 °A which agrees very well with that obtained from Figure B-10.

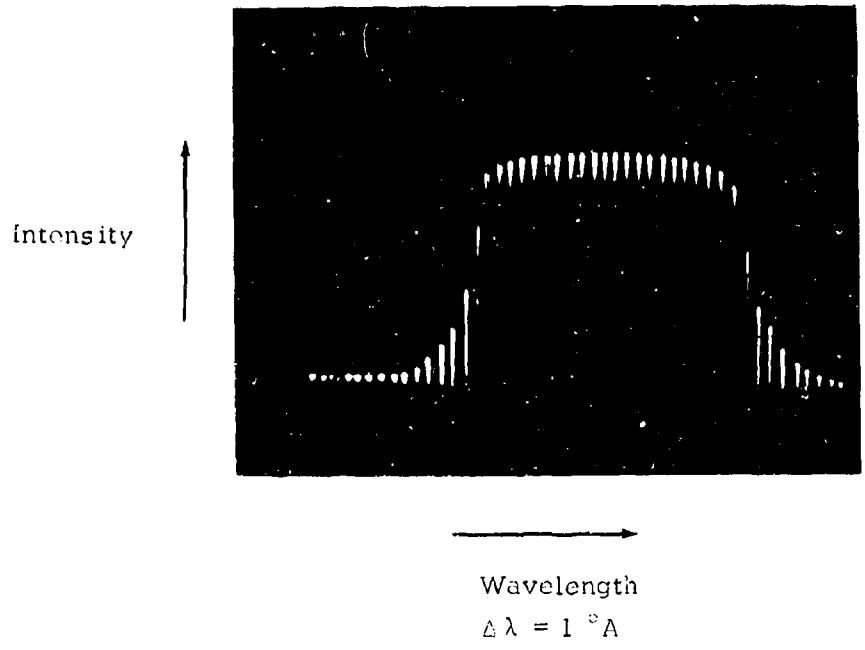


Figure B-10. Transmission Bandwidth for Mercury 2967 °A Line

UNCLASSIFIED

Security Classification

**DOCUMENT CONTROL DATA - R & D**

*(Security classification of title, body of abstract and indexing annotation must be entered when the overall report is classified)*

| | |
|---|---|
| 1. ORIGINATING ACTIVITY (Corporate author)<br>Dynamic Science, A Division of Marshall Industries<br>2400 Michelson Drive<br>Irvine, California 92664 | 2a. REPORT SECURITY CLASSIFICATION<br>Unclassified<br>2b. GROUP |

3. REPORT TITLE

COMBUSTION CHEMISTRY AND MIXING IN SUPERSONIC FLOW

4. DESCRIPTIVE NOTES (Type of report and inclusive dates)

Scientific Final

5. AUTHOR(S) (First name, middle initial, last name)

Stuart Hersh

| | | |
|---|---|---|
| 6. REPORT DATE<br>~~September~~ 1970 | 7a. TOTAL NO. OF PAGES<br>67 | 7b. NO. OF REFS<br>12 |
| 8a. CONTRACT OR GRANT NO<br>F44620-68-C-0069<br>b. PROJECT NO 9711-01<br>c. 61102F<br>d. 681308 | 9a. ORIGINATOR'S REPORT NUMBER(S)<br>DS TR A-70-103<br>9b. OTHER REPORT NO(S) (Any other numbers that may be assigned this report)<br>AFOSR 70-1873 TR | |

10. DISTRIBUTION STATEMENT

"1. This document has been approved for public release and sale, its distribution is unlimited."

| | |
|---|---|
| 11. SUPPLEMENTARY NOTES<br>TECH, OTHER | 12. SPONSORING MILITARY ACTIVITY<br>AF Office of Scientific Research (SREP)<br>1400 Wilson Boulevard<br>Arlington, Virginia 22209 |

13. ABSTRACT

Analytical and experimental investigations of the ignition and combustion of hydrogen-oxygen-argon mixtures are presented. A one-dimensional kinetics program with generalized chemistry and provisions for mass addition, momentum addition, heat loss, mixing, shock waves, and a rate screening option has been developed and used to analyze the effect of free radical additives on the ignition delay time in hydrogen-oxygen mixtures. This computer program has also been used to reduce shock tube measurements of hydrogen-oxygen ignition delay and $OH\ ^2\Sigma - ^2\Pi$ emission. The experimental results indicate that the reaction $O + H\ (+ M) \rightarrow OH^*\ (+ M)$ is responsible for producing $OH(^2\Sigma)$ during the induction period; however, this mechanism, when input into the computer program, was not sufficient to qualitatively reproduce OH emission intensity profiles obtained experimentally. Work aimed at determining the mechanism for OH emission throughout the reaction zone is continuing.

DD FORM 1 NOV 68 1473

UNCLASSIFIED

Security Classification

| 14 KEY WORDS | LINK A | | LINK B | | LINK C | |
|---|---|---|---|---|---|---|
| | ROLE | WT | ROLE | WT | ROLE | WT |
| Ignition Delay | | | | | | |
| Additive Effects on Ignition | | | | | | |
| Shock Tube | | | | | | |
| Chemiluminescence | | | | | | |
| Supersonic Combustion | | | | | | |
| Hypersonic Propulsion | | | | | | |
| Supersonic Ignition and Combustion Mechanisms | | | | | | |